ISSN 1173-5996

FIRE RESISTANCE OF LIGHTWEIGHT FRAMED CONSTRUCTION

BY

P.C.R. Collier

Supervised by
Associate Professor Andrew H Buchanan

Fire Engineering Research Report 00/2

March 2000

This report was presented as a project report
as part of the M.E. (Fire) degree at the University of Canterbury

School of Engineering
University of Canterbury
Private Bag 4800
Christchurch, New Zealand

Phone 643 364-2250
Fax 643 364-2758

Abstract

Limiting the fire spread through lightweight framed construction is a well established method of providing fire resistance. The objective is for the barrier to provide fire resistance for the required time, even if at the end of that time it has to be demolished, because of internal damage.

This report describes a software tool for predicting the likely fire resistance performance of a non-loadbearing or loadbearing wall subjected to a standard fire resistance test, or when subjected to real fire conditions.

Prediction of the performance of fire barriers in this study employed finite difference techniques for heat conduction within linings and also for convection and radiation on the boundaries and cavity. A user-friendly interface was developed for input of the parameters from the lining properties and dimensions, stud sizes, wall height and whether the studs are timber or steel. A choice of fire exposure is also permitted so that 'a standard ISO curve' or 'real fire with a decay period' may be input by the user. Algorithms for the charring of timber and reduction of steel strength and stiffness at elevated temperatures are included to determine a structural failure condition for the studs.

Acknowledgements

The research described in this report was conducted at the fire research facilities of BRANZ. The work was funded by the Public Good Fund of the Foundation for Research Science and Technology.

Acknowledgements are offered to:

Associate Professor Dr Andrew Buchanan, my supervisor, for proof reading drafts, technical advice and general guidance.

My employer BRANZ, for the opportunity to undertake the ME(Fire) programme, and allowing me to do this research project required for completion of the degree.

New Zealand Fire Service Commission for their financial contribution to the Fire Engineering Programme at the University of Canterbury.

Table of Contents **Page**

List of Figures

List of Tables

1 Introduction

1.1 Objective

The objective of this study is to incorporate data, methods and results from previous research into a standalone software package, where the user can specify a wall system and subject it to a time-temperature fire exposure and evaluate its performance. The choice of fire exposure is left to the user and this will enable the performance of system that already meets a particular fire resistance rating (FRR) to be assessed against a non standard (real) fire.

1.2 Background

In New Zealand, the fire resistance of barriers is determined by physical testing or by seeking an opinion from a fire expert or laboratory. The present environment requires extensive testing both for initial acceptance and as a means of gathering data to support variations by opinion. However, this normally limits the fire conditions to which barrier systems are exposed to standard (time-temperature) conditions. In practice, the actual heat fluxes impinging on wall surfaces vary considerably and depend on the nature and arrangement of fuel, thermal characteristics of room lining materials, the size of the room and the ventilation available. This will be essential input to the model proposed in this project, and this aspect will be addressed by work carried out at the University of Canterbury (Feasey, 1999) and another two research projects at BRANZ. Previous research at BRANZ has investigated the behaviour of plasterboard lined loadbearing timber and steel framed walls and this has resulted in the development of methods for extending the test results to design walls of different loadbearing capability and heights. Further work on a preliminary finite difference heat transfer model (Collier, 1996b) has confirmed the viability of this approach to solving the problem of non-standard fire scenarios as well as evaluation of design changes.

The work proposed will address some of the uncertainties in the behaviour of lining systems, timber and steel when subjected to fire. This includes taking into account the thermal breakdown of these materials such as cracking of linings which allows the passage of hot gases, and eventually exposes the wall framing to fully developed fire conditions. Certain linings such as gypsum plasterboard tend to ablate or erode over time during fire exposure. In past research, a temperature criterion has been used to determine how much of the lining has been eroded. This has not been entirely successful and refinements to a temperature criterion such as including the rate of temperature rise are a possibility.

The structural loadbearing ability of the timber framing will be modelled as the section size is reduced by charring. Similarly the loadbearing reduction of steel studs will be modelled.

The research will build on related work by other researchers and it is intended to develop self-contained user-friendly software as the primary vehicle for presenting the research results. The ready availability of a user friendly software model will enable designs to be evaluated in the heights and loads that may not be able to be evaluated in a furnace and/or in conjunction with non-standard fire conditions.

The proposed model will run in Microsoft Windows and is an important part of the technology transfer process because it will allow fire protection engineers and scientists to use results of research which involves complex mathematical calculations. Software will be made available for distribution on CD-Rom and from the Internet to ensure as wide as possible distribution in New Zealand and overseas. User and technical guides will also accompany the software, as well as other documentation in the form of journal or conference papers. This research is intended to facilitate performance-based design of barrier systems for situations especially where testing of the proposed design is either impractical or unnecessary, and which indirectly provides opportunity for optimising the design of fire separation and reducing costs.

1.3 Aim of this project

This project is scheduled to run over a period of four years and the stage at which this report is being prepared is at about one and three quarter years into the project. The progress to date is as follows:

- The principles of the finite-difference heat transfer model for the cavity wall systems under consideration have been developed using implicit equations and an inversion matrix procedure written to solve them.
- The thermal properties of gypsum as used by other researchers have been studied and an allowance for the inclusion of free moisture has been added to the data inputs of the model.
- Ablation of the lining is a significant milestone in the performance of a lining system and techniques for progressively removing sub layers of lining have simulated this process quite effectively.
- The model used for charring of the timber studs is based on the radiation received from the exposed lining; adjustments can be made for density, moisture content and oxygen depletion.
- A previously developed structural model based on the charring of the timber has been incorporated into the model, to reduce the loadbearing capacity as the stud is consumed by charring.
- With steel framed walls the temperature of the steel is the principal determinant of its strength and modulus of elasticity, modelling of heat transfer into the steel allows the reduction in loadbearing capacity to determined.
- The predictive capability of the model had been trialled against a variety of timber and steel fire resistance tests and a real fire compartment burn.

- A presentation of the model with a user-friendly interface and output graphics is operational.

Previous work at BRANZ (Collier, 1991a, 1991b, 1992, 1996a, 1996b, and 1999) (Gerlich, 1995a and 1995b) has established methods for extrapolating the results of loadbearing fire resistance tests to enable walls of greater loadbearing capacity and/or height to be designed. The methods published so far have relied on a fire resistance test as a basis for extrapolations and future designs are limited to that tested system only. There exists a need for a method with greater freedoms and flexibility, such as being able to deviate from the standard fire curve, to use alternative lining materials and add or remove insulation from the cavity. It is still however advisable to validate a basic lining system with a fire resistance test to ensure that it behaves as expected with regard to integrity, onset of char, and ablation. Other lining materials such as brick are straightforward to incorporate, especially since they have been baked in an oven and therefore do not have chemically bonded water to be driven off.

2 Finite difference model

Finite difference methods for determining heat transfer can be divided into two types, explicit and implicit. Equations for one, two or three dimensions may be constructed for solving heat transfer problems. For this study one-dimensional implicit equations were cast and solved using a matrix inversion method (Wade, 1998).

The implicit method has the advantage of being more stable, compared with the explicit method used in Collier (1996b). When using the explicit method the time step is sized so that several inequalities involving the Fourier and Biot numbers are satisfied. If these limits are exceeded instability results which generates large positive and negative values such that temperatures diverge. The solution is in setting smaller and smaller time steps to maintain stability, but the downside is that execution speed becomes very slow to the point where the programme appears to have totally locked up. With implicit equations, instability and slow execution are largely avoided, some inaccuracies in the calculations are inherent if time steps are too large but realistic limits on time steps will produce accurate results in a reasonable execution time.

The finite difference model developed in this study is a compilation or several component parts, which make up a cavity wall. For the lining layers it is a heat transfer by conduction problem, complicated by the changing properties - with temperature - of the lining. Heat transfer in the fluid spaces is by convection and radiation. When the lining cavity is filled with insulation, then it becomes a conduction calculation. Strictly speaking heat transfer in the insulation is by convection and mass transfer (Gammon,1987), but due to the complexities of the algorithms involved, reducing the problem to one of conduction is a justified simplification.

All the way through the execution of the programme, values for physical properties are updated according to the temperature of that particular part of the assembly.

2.1 Principle of finite difference method as applied to a single slab

To illustrate the application of the FD method a single slab (of plasterboard or other suitable material) is illustrated in Figure 2.1. A finite-difference grid was applied to the lining, dividing into 4 slabs (5 nodes, coarse grid) or 8 slabs (9 nodes, fine grid).

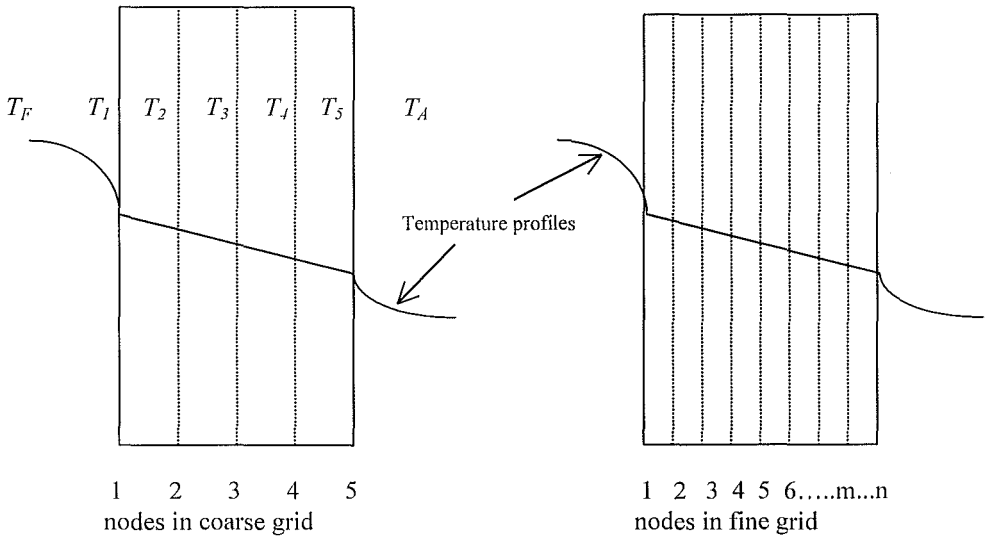

Figure 2.1: Applying finite-difference grids to coarse and fine slabs with fire exposure on one side

The heat transfer is described in implicit one-dimensional equations in equations 2.1 to 2.4. The subscripts on the temperatures T refer to the node position, F and A refer to the fire and ambient nodes respectively, while numbers 1,2,3, ...m, .n refer to nodes within the slab. The superscript p refers to the time, and $p+1$ is the next time. Within the slab heat transfer is treated solely as a conduction problem, moisture transport can be ignored. Moisture transport originating from the evapouration water of hydration is not modelled. This simplification is possible when it is considered that the moisture, although in reality it evapourates and condenses several times onto cooler surfaces before those surfaces heat up and it evapourates again, the net effect is that from an enthalpy consideration it is only evapourated once. On the fluid interfaces of the slab, heat transfer is by a combination of radiation and conduction as described in Equation 2.1 where the Biot No

Bi in equation 2.3 is dependent on h, an overall heat transfer coefficient in equation 2.7, which is derived from the convective and radiative coefficients in equation 2.8 and 2.9.

$$(1+2\mathrm{Fo})T_1^{p+1} - 2\mathrm{Fo}T_2^{p+1} = \frac{2\mathrm{FoBi}(T_F - T_A)}{h} + T_1^p \qquad \textbf{Equation 2.1}$$

Where the Fourier and Biot numbers are given by:

$$\mathrm{Fo} = \frac{\alpha \Delta t}{(\Delta x)^2} \text{ with } \alpha = \frac{\mathrm{k}}{\rho \mathrm{c}} \qquad \textbf{Equation 2.2}$$

$$\mathrm{Bi} = \frac{h\Delta x}{k} \qquad \textbf{Equation 2.3}$$

h is defined in equations 2.7, 2.8 and 2.9.

The implicit form of the interior node is given by Equation 2.4:

$$-\mathrm{Fo}T_{m-1}^{p+1} + (1+2\mathrm{Fo})T_m^{p+1} - \mathrm{Fo}T_{m+1}^{p+1} = T_m^p \qquad \textbf{Equation 2.4}$$

Solution of the simultaneous implicit equations at each time step is performed by the matrix inversion method by expressing the equations in the form [A][T]=[C], where:

$$[\mathrm{A}] = \begin{bmatrix} 1+2\mathrm{Fo} & -2\mathrm{Fo} & 0 & 0 & \cdots & 0 \\ -\mathrm{Fo} & 1+2\mathrm{Fo} & -\mathrm{Fo} & 0 & \cdots & 0 \\ 0 & -\mathrm{Fo} & 1+2\mathrm{Fo} & -\mathrm{Fo} & \cdots & 0 \\ \vdots & \vdots & \ddots & \cdots & \cdots & \vdots \\ 0 & \cdots & \cdots & 0 & -2\mathrm{Fo} & 1+2\mathrm{Fo} \end{bmatrix} \qquad \textbf{Equation 2.5}$$

$$[\mathrm{C}] = \begin{bmatrix} 2\mathrm{FoBi}_F(T_F^P - T_1^P)/h + T_1^p \\ T_2^p \\ T_3^p \\ \vdots \\ 2\mathrm{FoBi}_A(T_A - T_n^p) + T_n^p \end{bmatrix} \qquad \textbf{Equation 2.6}$$

The bottom rows of [A] and [C] represent the ambient interface and are basically mirror images of the fire interface.

The above treatment is a simple application of a finite difference as applied to a single slab or lining. The basic method is reproduced over again for more than one lining, usually with fluid interfaces on each side where a cavity is such an example.

2.2 Extension to a cavity wall system

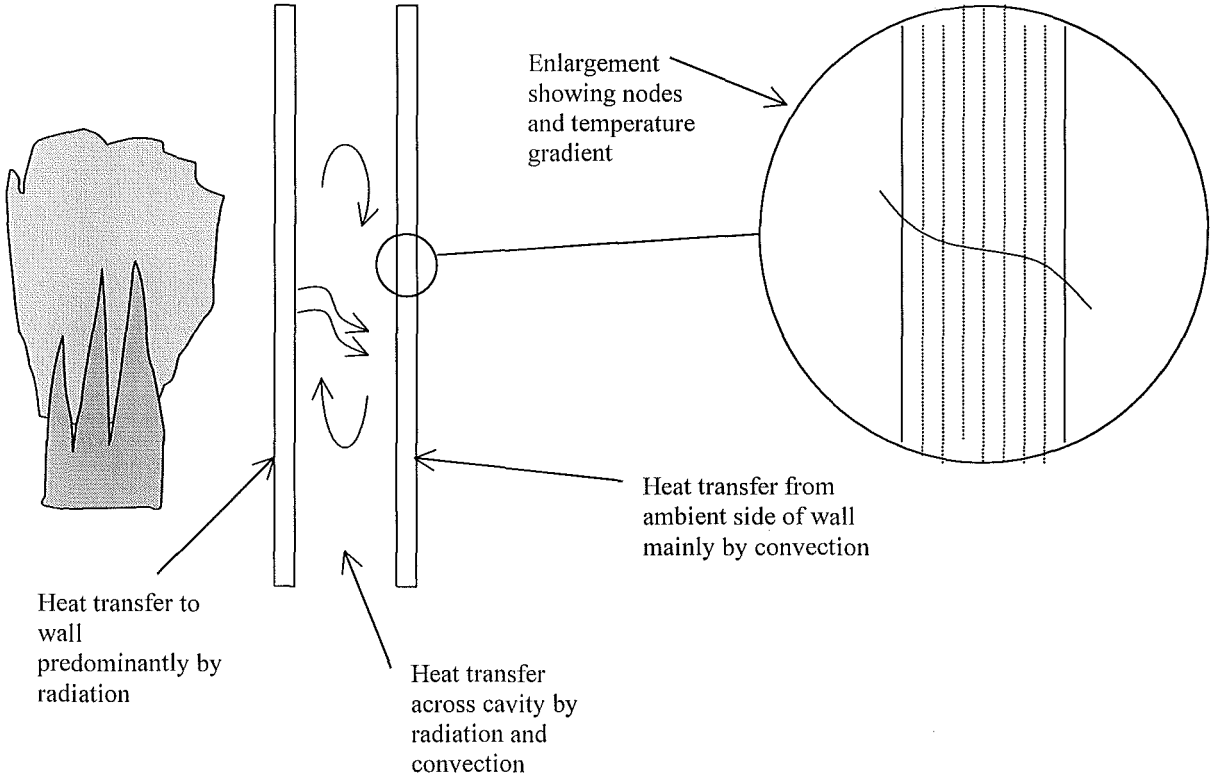

Figure 2.2: Application of finite difference techniques to a cavity wall in combination with radiation and convection

Modelling of the fire side, ambient side and cavity requires consideration of heat transfer by radiation and convection (Collier 1996b). When temperatures are low heat transfer by convection will dominate, as the temperatures rise the proportion of heat transfer by radiation will increase.

The equations 2.1 to 2.6 describe the boundary conditions; values for Bi can be determined by h and k depending on the formulations below

$$h = h_c + h_r$$ **Equation 2.7**

where, the convective coefficient is given by: (Rogers, 1972)

$$h_c = 1.31(T_F - T_1)^{0.33}$$ **Equation 2.8**

and, the radiative coefficient is given by:

$$h_r = \varepsilon\sigma(T_F + 273 + T_1 + 273)\left((T_F + 273)^2 + (T_1 + 273)^2\right)$$ **Equation 2.9**

A sensitivity analysis of heat transfer coefficients by Thomas (1997) is discussed in section 2.5.

Handling the heat transfer across a cavity can be tackled in several ways TASEF (Sterner, 1990) considers a simple radiation exchange and the temperature of the cavity. Collier (1996b) compared a simple radiation exchange and a more complex solution where the fluid receives heat by radiation and convection from the hot surface, increasing in temperature in the process, and then transfers heat to the cooler surface by the same mode. After comparing the merits of the two modes the latter was adopted and that method has also been used in this project.

2.3 Multiple layers of lining

Interfaces between linings in multiple layer systems can be handled using the method described below (Croft, 1977) and illustrated in Figure 2.3. Ideally this is a case of steady conduction across a thin interface, where there is an apparent temperature discontinuity. The fictitious interface temperature drop ΔT_{int} is found by extrapolations of the local linear temperature profiles in each material just away from the contact disturbance.

With steady heat flux

$$Q''_{AB} = -k_A \frac{\partial T}{\partial x}|_A = -k \frac{\partial T}{\partial x}|_B$$ **Equation 2.10**

and the unit interface conductance is

$$h_i = \frac{Q''_{AB}}{\Delta T_{\text{int}}} \qquad \textbf{Equation 2.11}$$

In the ideal case of perfect contact, the temperature drop ΔT_{int} vanishes and $h_i \to \infty$; then there is temperature continuity $T_A = T_B$ at the interface but perhaps a discontinuity in the temperature gradient, since $k_A \neq k_B$ if the linings are different.

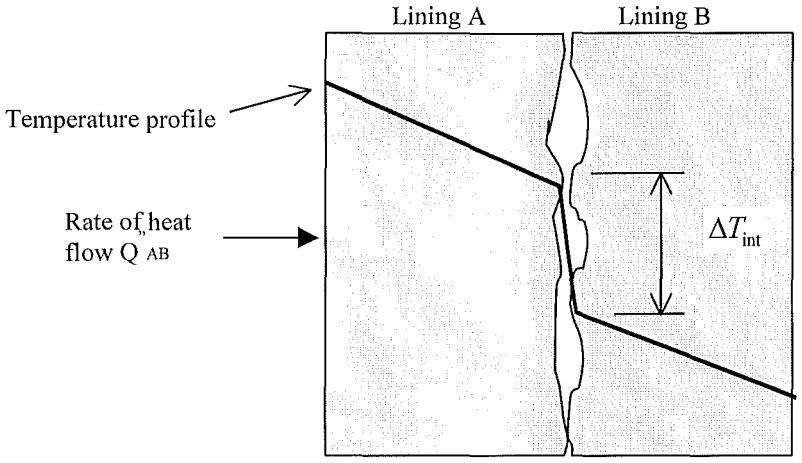

Figure 2.3: Temperature profile across a typical interface

Finite difference equations can be derived the same way as for boundary nodes with convective (and radiative) conditions, but for the purposes of this model a simplification was employed empirically for the case of two sheets of lining touching (or almost) each other. A realistic value of h_i was determined, by trial and error, to match the test results. The trials showed that the sensitivity to variations in h_i is not significant for a sensible range of values.

2.4 The addition of insulation

With insulation in the cavity, changes to the heat transfer method from convection and radiation to a net assumption of a conduction type regime offers a viable means of modelling the situation. An explanation of the reasoning behind this follows.

The mode(s) of heat transfer through insulating materials is complex and seemingly there is a different answer for each type of insulation. Gammon (1987) explains that most insulating, materials are porous. The pore system can be closed, such as in wood and cellular plastics, or open, as in mineral wool. In a closed system, heat transfer can occur by radiation and gas conduction in the pores, as well as solid phase conduction. In open pore systems heat transfer can additionally occur by natural or forced convection, and therefore depends on whether the material is oriented horizontally in service.

The basic equation for heat flow in a porous medium, Darcy's law, relates mass flow to pressure gradient by the permeability. In fibrous materials, anatomical anisotropy results in at least two permeabilities, parallel and perpendicular to the fibres. Since practical applications are complex, semi empirical solutions offer a possible solution.

In the case of fibreglass the thermal conductivity is a function of temperature, generally increasing with temperature. Radiation effects, which become pronounced at higher temperatures, are shown as a rise in conductivity at higher temperatures. Product literature, which shows the variation of the thermal conductivity, may be used as an input to the model. If this data is available then heat transfer across the cavity can be treated as a conduction problem, albeit when some assumptions are made about heat transfer across the lining to insulation interface. This has not been incorporated in the model at this stage.

Product literature (Rockwool as an example) gives a graph of conductivity *Wm/k* vs temperature and the graph terminates at the maximum service temperature as specified by the manufacturer. Beyond this temperature it is assumed that the insulation has melted or is otherwise no longer capable providing the service originally intended.

2.4.1 Various types of insulation

Type of insulation range from the extremes of fibreglass, which melts at a relatively low temperature, to mineral types that don't melt.

Irrespective of the type of insulation the exposed lining is subjected to a more severe temperature exposure while the insulation remains in place throughout the cavity. This is because the transmission of heat through the cavity is impeded, resulting in a build up of heat and temperature in the exposed lining. The elevated temperature will cause more rapid deterioration of the exposed lining, this effect can be significantly mitigated if the lining is a fire rated type which commonly includes fibreglass in the core to reduce/delay cracking of the lining and eventual detachment from the framing. Once the lining has fallen off the cavity is then exposed to the full fire exposure conditions, the fibreglass if it hasn't already melted probably will at this stage.

Conditions where the inclusion of insulation will improve the performance of the wall require the exposed lining to remain in place and it is assumed that the insulation does not melt or shrink during the same period. Heat transmission through the assembly is impeded and while this situation prevails failure by the insulation failure criteria or temperature rises on the ambient side are impeded. Extension of this philosophy to the studs, whether they are timber or steel, for insulation that remains in close contact with the sides of the studs, affords some protection against heat input into the studs as long as it remains in place. The exposed face of the studs, will heat up in a similar scenario to the case where there is no insulation.

If the insulation shrinks when heated and a gap between the studs and insulation opens up, the channel created can trap the heat flow against the studs and subject the sides of the studs to higher temperatures than if there was no insulation at all.

2.5 Radiation and convection coefficients

Thomas (1997) performed an extensive sensitivity analysis of the radiation and convection coefficients by demonstrating the effect on wall surface temperature and net heat flux to the wall of high, low and mean values. The results of the study in general showed in most cases a relative insensitivity to quite wide variations in the coefficients. The final values selected by Thomas (1997) are in the middle of the range as listed in Table 2.1.

Where ε is the effective emissivity for radiation heat transfer as given by equation 2.9

$$q'' = \varepsilon\sigma T^4 \qquad \textbf{Equation 2.12}$$

while β and γ are the coefficient and index in equation 2.8.

$$h = \beta(T_g - T_s)^{(\gamma-1)} \qquad \textbf{Equation 2.13}$$

In equation 2.8 the value of β was 1.31, as was shown by Thomas (1997) the overall results are not greatly sensitive to this value.

Table 2.1: Heat transfer coefficients

Position	ε	β	γ
Fire Side	0.8	1.0	1.33
Lining, Fire Side of Cavity	0.6	1.0	1.33
Lining, Ambient Side of Cavity	0.6	1.0	1.33
Wood Stud Side of Cavity	0.6	1.0	1.33
Ambient Side	0.6	2.2	1.33

3 Thermal properties of common lining materials

3.1 Gypsum plasterboard

Gypsum plasterboard linings are commonly used to provide fire resistance in framed construction. When exposed to fire the free water and chemically combined water in the gypsum is gradually driven off at temperatures above 100°C. This causes a temperature plateau on the unexposed face of the lining. The length of this plateau is a function of the lining thickness, density, composition and also the percentage of free moisture. As temperatures rise above 100°C, calcination of the gypsum plaster severely reduces its strength. At room temperature screw-fixed gypsum plasterboard linings provide adequate restraint against lateral buckling of the studs about the minor axis. During exposure to fire this ability to provide lateral restraint diminishes as the thickness of undamaged gypsum progressively decreases.

When the temperatures on the hot side of the wall assembly reach critical levels the exposed plasterboard lining will no longer provide lateral restraint. In comparison the lining on the cold side of the assembly will degrade to a lesser degree, and its ability to provide lateral restraint will depend on the remaining thickness of undamaged material.

Thomas (1997) evaluates data measured by Mehaffey et al (1994), Andersson et al (1987) and Harmathy (1988) for the thermal conductivity and enthalpy of glass-fibre reinforced gypsum plasterboard as a function of temperature. Thomas' values for the enthalpy of gypsum plasterboard are presented in Figure 3.1 along with a selection from other researchers. The enthalpy values presented in Figure 3.1 and represent the summation of the product of specific heat and temperature. Enthalpy values are used in modelling to avoid numerical instabilities resulting from the sharp peaks that may occur in the specific heat of materials containing water, due to evaporation of moisture.

Alternative sets of enthalpy data for gypsum plasterboard were obtained from Fuller (1992), Cooper (1997), Sultan (1996) and Perry (1997) and these are compared with Thomas' (1997) values and are included in Figure 3.1. Thomas' data has been converted from a kJ/m^3 basis to kJ/kg using a density of 510 kg/m^3 for purposes of comparison. The values used by Fuller for enthalpy are generally higher up to about 300°C, especially in the region of the spike around 100°C where moisture is evaporated. This can be attributed to Fuller using a moisture content of 7% for the free water in the gypsum, a value higher than the 1-2% commonly found in BRANZ commercial testing and Thomas' quoted range of 4-8%. The enthalpy of gypsum is quite sensitive to the value of free moisture chosen.

Variations in the moisture content can affect the model results quite significantly and a sensitivity analysis is presented in section 6.1 and the relative performance between the model and the test results is compared on Table 6.2.

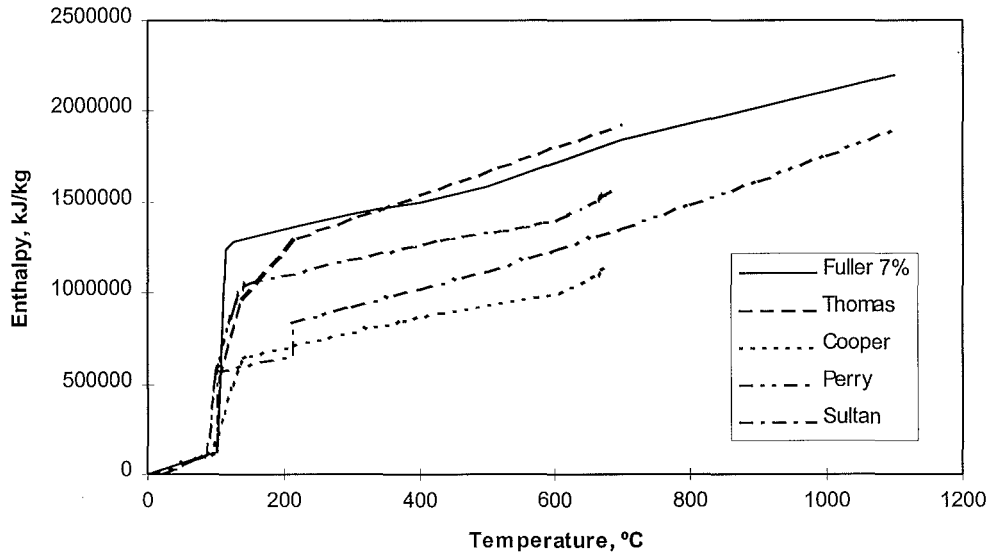

Figure 3.1: Enthalpy vs temperature

For Fullers' enthalpy data, which is used in the model, it was necessary to be able to vary the moisture content from 0 to 7% and higher if necessary. Figure 3.2 shows a family of curves, which illustrate the proportion of the range of enthalpy attributable to the free moisture. These values where obtained by removing the contribution of the 7% of free moisture contribution to the spike at 100°C and then putting it back in on a pro-rata basis according to the moisture content.

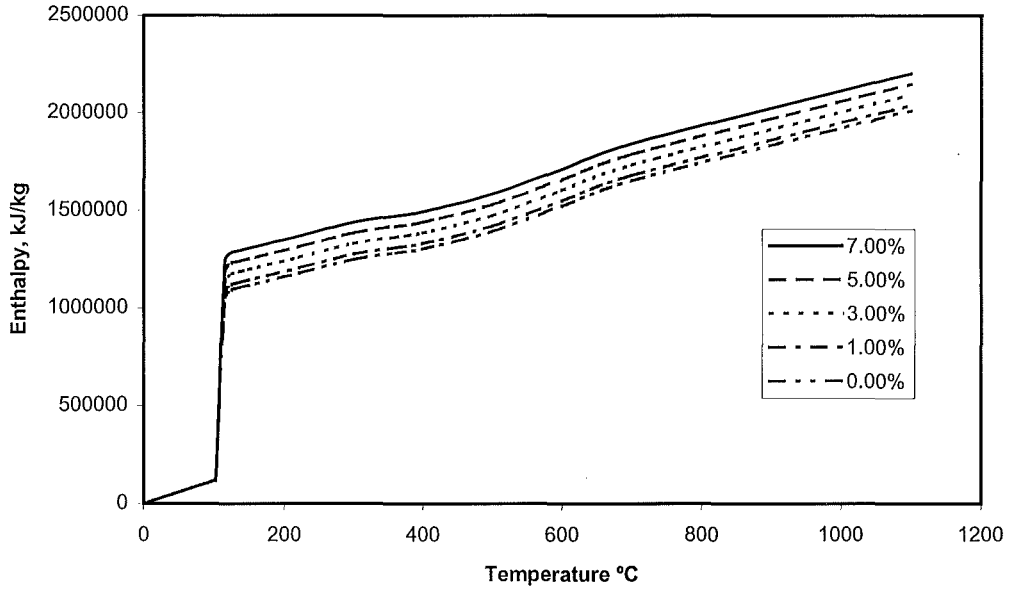

Figure 3.2: Variation of enthalpy with moisture content

For density and conductivity the values used by Fuller (1992) are typical of those used by other researchers and are presented in Table 3.1. In the context of this study the values of density were taken as relative, and used as a basis for the changes in the density of a measured sample that may have been 797 kg/m^3 (in the case of 12.7 mm plasterboard) initially and reduced proportionally with temperature.

Table 3.1: Density and conductivity of gypsum

Temperature, ^{o}C	Density, ρ, kg/m^3	Conductivity, k, $Wm^{-1}K^{-1}$
25	678	0.25
98	651	0.25
100	651	0.25
103	648	0.25
115	646	0.25
125	644	0.25
200	642	0.13
300	638	0.13
360	642	0.13
400	641	0.13
500	638	0.13
600	632	0.13

3.1.1 Ablation of lining

Thomas (1997) describes ablation is a process whereby consecutive layers of a material are shed as a material undergoes heating. This occurs because the material undergoes chemical and physical changes during heating which reduces the bonding of the material to itself. The material then tends to fall away because it is not firmly attached to the material underneath. As gypsum is heated it is transformed into calcium anhydrate, has the appearance of a dry cohesionless powder, which will then fall off the unaffected board. If the powder is not lost in this process, the shrinkage of the gypsum causes fissures to penetrate into the core, increasing the path for heat transfer. This process is slowed if the board is reinforced with fibreglass, which improves cohesiveness and increases the temperature that ablation occurs.

The temperatures for which ablation occurs range from 500 to 700°C for standard gypsum board. For glass fibre reinforced boards gypsum plasterboards, generally known

as fire-rated boards, the ablation range is 700 to 900°C. The effect of ablation is more apparent when comparing the results of boards of different thicknesses ablation has a more serious effect on a thinner board due to the fact that a higher proportion of the board is lost.

In terms of modelling the effect of ablation, a method (Gammon, 1987) that has been trialled with some success is to remove from further consideration layers of lining that have exceeded the ablation temperature. At the end of each time step when the temperature of each element (between nodes) has been evaluated, those elements that exceed the ablation temperature are eliminated from further consideration, so the lining is gradually thinned out by this means of simulating ablation. Attempts to simulate cracking of the lining, by means of increasing the conductivity were not successful and were abandoned.

3.2 Brick

The behaviour of brick is quite different to gypsum; no spike in specific heat is encountered when water of hydration would normally be driven off. This is because bricks are baked in oven as part of the curing process, so brick is essentially anhydrous, any free moisture is not normally considered. Concrete bricks however behave similarly to gypsum, since the curing process is similar.

Wall systems with brick on one face for external exposure are similarly treated as a cavity wall, where the bricks are treated as one of the linings. The prevailing physical properties of the brick will dictate the performance and can be entered as inputs, from actual measurements of the bricks used for density, specific heat (assumed constant) and conductivity from the best information available such as in Perry's (1997) Chemical Engineers handbook).

3.3 Wood composite

Wood and wood composite may be modelled as a barrier. The behaviour is similar to gypsum, as there some free moisture to evaporate. The structure breaks down or chars at 300°C or sooner for a wood composite with some particular (heat affected) glues as the binding agent. Once the temperature has exceeded 300°C on the unexposed side of a barrier, it is deemed to no longer be present.

3.4 Concrete

Concrete was included in the earlier stages of the study as sometimes construction systems have been encountered where a concrete slab was covered with a sheet of plasterboard or similar on one or both sides.

The exact properties of concrete were not required in these instances because a fire resistance test result was available and estimates of the physical properties were then input into the model on a trial and error basis until a match with the test result was obtained. Having established reasonable agreement with the test result, modifications to the system, such as the addition of plasterboard to concrete could be trialled to establish the probable improvement.

Thermal properties for various concrete aggregates at elevated temperatures can be obtained from Buchanan (1999) and Schneider (1988).

4 Structural model for timber

The structural model used in the software is based on the method resulting from the previous research, as the wall being modelled is subjected to the fire the loadbearing capacity is reduced with respect to time of the fire exposure. The time of structural failure can be determined as when the loadbearing capacity reduces below the applied load.

4.1 Charring of timber studs in cavity

When the studs in the cavity of the wall begin to char, at a time when the temperature of the cavity side of the exposed lining exceeds 300°C, the resulting loss of stud section reduces the loadbearing capacity. Previous research by the author (Collier, 1991a, 1991b, 1992, 1996a and 1999) established a relationship between the depth of char, referred to as "charfactor" and a likely distribution of the remaining cross-section, and the loadbearing capacity for the particular initial stud dimensions and wall height.

4.1.1 Radiation model inside the cavity

If it is considered that the cavity side of the exposed lining behaves as a radiation source, then the resulting radiation from the lining will impinge onto the timber stud, and cause charring at a rate according to equation 4.1. The actual level of radiation reaching the stud will depend on the view factor at each particular location of the stud. For the face of the stud attached to the exposed lining, this can be treated as a radiation problem with two parallel surfaces. Even if the surfaces are essentially in contact, it is still considered heat transfer by radiation, with a view factor of 1.0. The sides of the stud are exposed to the same radiator at right angles, the distance between studs being the width of the radiator and the depth being the space between nogs. The configuration factor is relatively insensitive to changes in dimensions of the radiator beyond the stud and nog spacings, but theses values are used for convenience in setting the radiator size. Because of a reducing exposure the further from the lining, the sides are expected to char less

towards the unexposed lining. The exposed corners of the stud are expected to char at an increased rate due arris rounding, which is effectively to a double exposure, BS 5268 (1987), and where the radius is equal to the char depth.

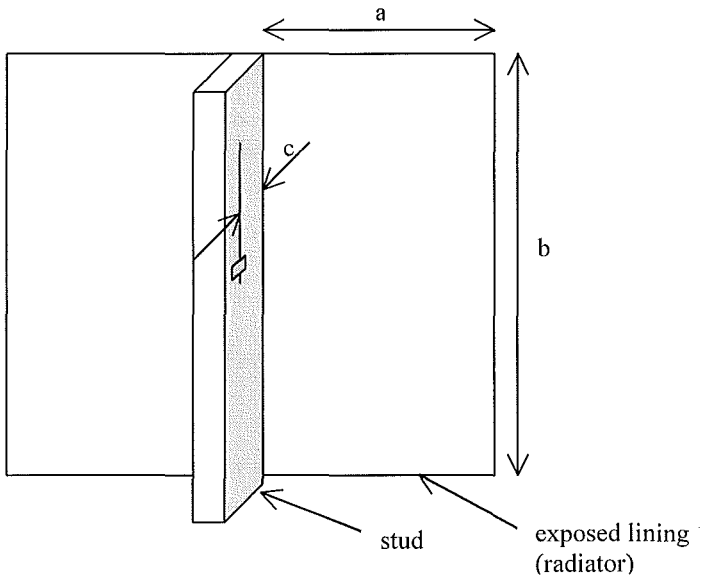

Figure 4.1: Exposure of stud to radiation from lining

Figure 4.1 shows the basis for calculation of the configuration factor – formulations (Tien et al 1995) for exposure where the receiver is perpendicular to the radiator where:

$$X = a/b,\ Y = c/b,\quad A = 1/\sqrt{X^2 + Y^2} \qquad \textbf{Equation 4.1}$$

where a = between studs spacing , b = between nogs spacing, c = distance from exposed face

$$\phi = \frac{1}{\pi}[\tan^{-1}(1/Y) - AY\tan^{-1}A] \qquad \textbf{Equation 4.2}$$

and the incident radiation at point a is given by :

$$\dot{q} = \varepsilon\phi\sigma T^4 \qquad \textbf{Equation 4.3}$$

where ε = emissivity, ϕ = configuration factor, σ = Stephan - Boltzman constant and T = absolute temperature of the exposed lining

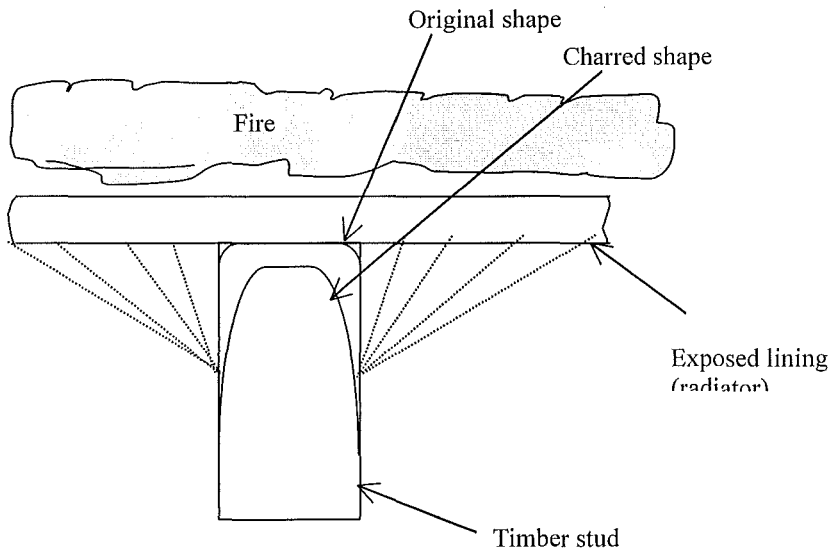

Figure 4.2: Cross-section view of radiation exposure on stud

Figure 4.2 shows a representation of the radiation impinging on the sides of the stud and an approximate charring profile.

A further refinement was considered where the contribution of the cooler un-exposed lining is also modelled and in fact would have the net effect of taking heat away from the stud. This would be more complex because the temperature of the stud would need to be known. Further development of this particular approach was abandoned when it was apparent that the additional charring resulting was minimal.

A radiation induced char model (Butler, 1971) on the basis of the incident char impinging on the stud surfaces causing char and loss of (surface recession) of stud. Butler demonstrated that the charring rate is proportional to the radiation such that:

$$Char\ rate = 21.96\dot{q} \quad \text{mm/min.}$$

where q is the radiation in MW/m^2

Equation 4.4

Mikkola (1990) supports Butler's finding that the charring rate is proportional to the external heat flux.

Further adjustments to the charring rate can be based on density, moisture content and oxygen concentration can be included based on the method developed by Mikkola (1990) and described as follows.

Charring rate is approximately inversely proportional to the density of the timber and a relative relationship is presented by

$$\beta \sim (\rho + 120)^{-1} \qquad \textbf{Equation 4.5}$$

where β and ρ are the charring rate in mm/min and the density in kg/m^3 respectively.

Charring rate is reduced by increases in moisture content according to

$$\beta \sim \frac{1}{(1+2.5w)} \qquad \textbf{Equation 4.6}$$

where w is the moisture content given by

$$w = \frac{m - m_o}{m_o} \qquad \textbf{Equation 4.7}$$

where m and m_o are the mass of a wood sample and the mass of the same wood sample after oven drying.

Reducing oxygen content, as a fire progresses, also has the effect of retarding the charring rate. A reduction from 21%, as in ambient air, which is also the environment in a cone calorimeter exposure, down to 8–10% as would be encountered in a fire resistance test results in the charring rate dropping by approximately 20%. In a fully developed fire the oxygen content may drop to zero in which case the charring rate could reduce by 35 to 50%. The environment in the cavity of a timber-framed wall may vary within the range covered above as the timber chars/combusts, as a result predicting the char rate is further complicated.

4.1.2 Finite difference model

A charring model based on heat transfer into the stud by radiation/convection and conduction within, was trialled using a two-dimensional finite difference technique. Properties for timber at elevated temperatures were obtained from Fuller (1992), and essentially the major influence on heat transfer is density, which reduces significantly above 300°C.

While it was shown that this model was able to reliably to predict the charring rate and the profile of the remaining stud, the execution time when using a fine enough grid of nodes to produce meaningful data was so long that it was not considered worthwhile using in the software. Further development was dropped in favour of the radiation model in 4.1.1.

4.2 Reduction of loadbearing capacity with charring

4.2.1 On basis of charring as used in BRANZ technical recommendation 9

BRANZ Technical Recommendation TR9 (Collier, 1992) uses the charring of studs as a basis for a reduction in the loadbearing capacity of the studs. The principles of TR9 are embodied in two versions of software to perform the same calculation (Collier, 1996a and 1999), whereby the result of a prototype test is used to forecast the performance of a similar wall (same lining configuration) on the basis of the stud size, height and load for the same fire exposure time or charfactor.

The studs in a light timber framed wall, when subjected to fire, are modelled as axially loaded columns. The effect of fire is simulated by the loss of timber cross-section in the studs and a calculation of the residual loadbearing capacity. The "Secant Formula" is applied to what is assumed, to be eccentrically loaded studs (in a wall) and has been

modified to include the effects of charring of the studs and face loading due to lateral forces.

The equation describing the stresses in the studs is a modified version of the "Secant formula" as used in Collier (1991a) and is as follows:

$$\sigma_{max} = \frac{P}{A}[1 + \frac{ec}{r^2}\sec(\frac{\alpha L}{2})] + \frac{M(D - C)}{2I} \qquad \textbf{Equation 4.8}$$

where :

σ_{max} = maximum permissible stress, N/m^2

P = axial load per stud, N

A = (D - C)(B - C), residual cross - section area of stud, m^2

D = depth of stud, m

C = char depth in stud (or charfactor, see definitions below), m

B = breadth of stud, m

$e = \frac{C}{2} + X$ actual eccentricity of loading , m

X = initial eccentricity of loading, m

$c = \frac{D - C}{2}$,

r = 0.289(D - C), radius of gyration, m

$\alpha = \sqrt{\frac{P}{EI}}$

$I = \frac{(B - C)(D - C)^3}{12}$, second moment of area, m^4

E = modulus of elasticity of the timber, N/m^2

L = height of stud, m

M = bending moment due to face pressure, Nm

A prototype fire resistance test on a loaded wall is required to establish the performance of the lining system and timber frame in terms of the criteria of stability, integrity and insulation. The test result will also enable the charfactor (degree of damage to the wall) to be assessed.

Definition of charfactor:

The charfactor is as a special case of char depth, as is illustrated in Figure 4.3 and applied to equation 4.8. It is based on an assumption that the char depth on the sides of a stud is half that of the face towards the exposed lining.

The concept of charfactor is applied as follows.

Step 1

The charfactor as the measure of fire damage is determined from a prototype test and is an arbitrary amount of char required for structural failure at the applied load in accordance with equation 4.8. The charfactor so determined is relevant only to the lining system tested at the time that the structural failure occurred.

Step 2

The charfactor can be considered as a unique number that is applied to the new (extrapolated) design to assess its probable performance. The new design has the freedoms of height and stud size and the expected loadbearing capacity is determined using equation 4.8.

The concept of charfactor as described above has been validated by Collier (1991a and 1992).

In the software under development the reduction in loadbearing capacity of the studs is continually assessed using a modification of steps 1 and 2 above. Instead of testing (step1) a wall to determine the charfactor, it is continuously calculated on the basis of the radiation exposure in 4.1.1 and equations 4.1 to 4.7. An iterative procedure (step 2) is used to calculate the loadbearing capacity since it occurs in two places on the left hand side of equation 4.8, as P and α. At this stage the bending moment due to face pressure has been omitted, because it has previously been shown to have a minor effect on the final result.

Simulation proceeds comparing the applied load with the residual loadbearing capacity based on the depth of char in the stud. The loadbearing capacity reduces with respect to time, and a failure point can be predicted when the loadbearing capacity falls below the applied load.

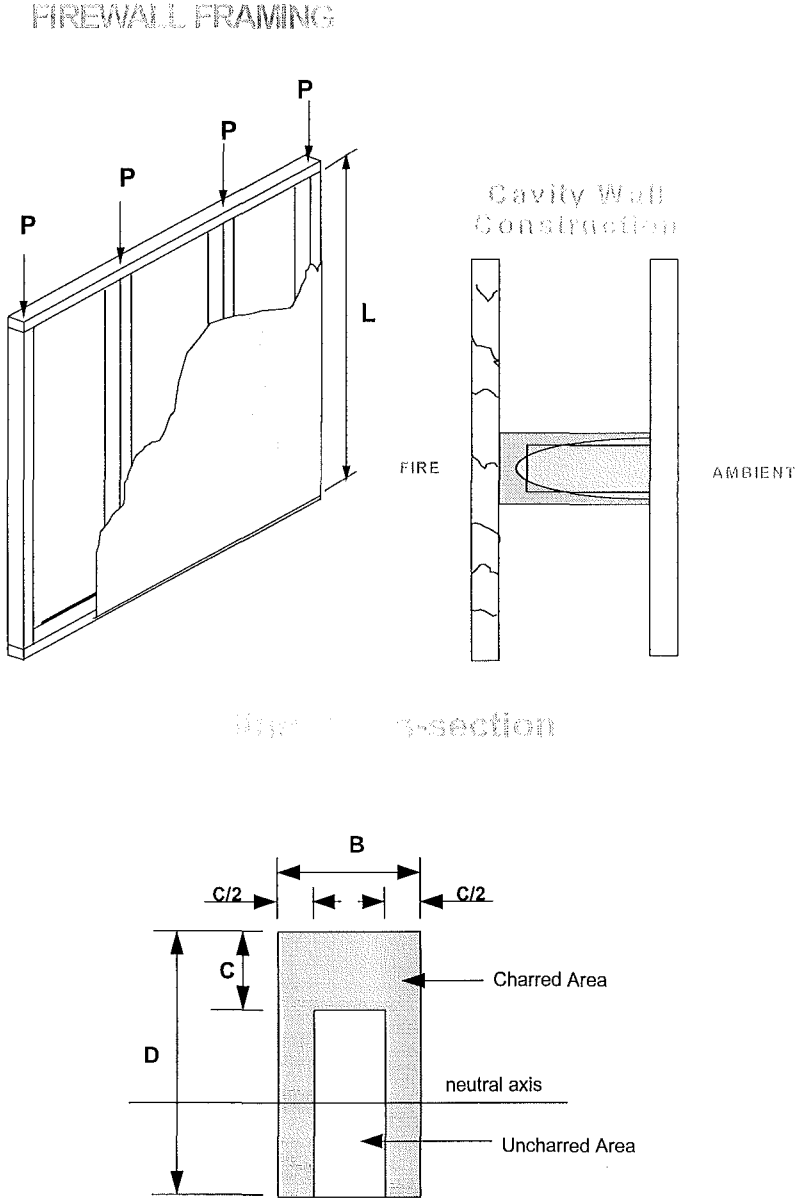

Figure 4.3: Loadbearing wall and charring of stud

5 Structural model for steel

5.1 Heat transfer in steel frame

Heat transfer in the steel studs was attempted using two methods, finite difference analysis and lumped thermal analysis.

5.1.1 Finite difference analysis

A finite difference analysis to model the temperature distribution in the steel studs was trialled. Heat input was by conduction from the exposed lining to the adjoining flange and to the web by convection and radiation. This approach proved to be unsuccessful for the following reason. The high conductivity k of the steel contributes to a high Fourier Number (Fo) (refer to equation 2.2), which in turn requires very small time steps so that the Fo maintains a value of approximately 0.5; otherwise the results obtained are not reliable. It was stated earlier in section 2.0 that the use of implicit equations has the advantage of being unconditionally stable, while performing the same calculation using explicit equations would result in instability if Fo ≥ 0.5. If implicit equations are used and Fo exceeds 0.5 even if instability is not apparent, which is usually obvious if values (such as temperatures) begin to oscillate between extreme negative and positive values, the quality and reliability of the calculation cannot be assured. Alternatively increasing the distance between nodes Δx (resulting in a coarse grid) to counter the effect will also degrade the quality of the result and in any case for a thin steel section there is little scope for increasing the grid size. Either way the end result is a slow programme execution and meaningless results because of the coarse grid. For these reasons further development of this approach was curtailed and an alternative sought.

5.1.2 Lumped thermal analysis

A more viable alternative is to consider heat input into the stud by convection/radiation on the web and conduction on the flange (see Figure 5.1). Heat transfer into the web can be treated as a lumped heat analysis on a thermally thin material. Where the temperature rise of the stud due to cavity convection and radiation is given by:

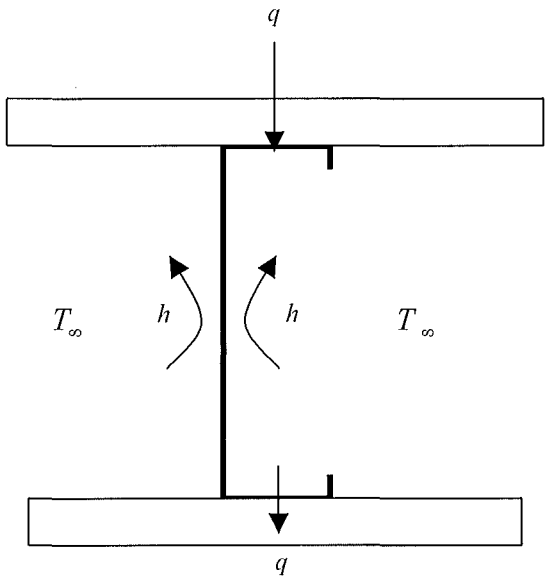

$$\frac{T_\infty - T}{T_\infty - T_o} = \exp\left(-\frac{2ht}{L\rho C_p}\right)$$

where :

T_∞ = cavity temperature

T = steel temperature

T_o = initial steel temperture

h = convection/radiation coeficient

t = time

L = steel thickness / 2

ρ = steel density

C_p = specifirc heat of steel

q = heat flow into and out of flanges

Figure 5.1: Lumped thermal analysis

For conduction the entire stud is modelled as a thermal bridge between the exposed (hot) and unexposed (cold) linings. Heat enters the stud on the exposed flange and exits on the unexposed flange and consequently generates a temperature difference across the stud. Modelling trials of this approach indicated that there appears to be some additional resistance to the heat flow at the lining/stud interface. Croft and Lilley (1977) explore this phenomenon and conclude that an air gap effectively exists at the lining stud interface, although the two surfaces are essentially in contact, where the two surfaces are essentially rough and not in total contact as shown earlier Figure 2.3. This is treated as

an interface where the heat transfer is by convection, the convection coefficient h_c was determined by trials and a value of 10 W/mK delivered close agreement with experimental results.

Further analysis of this thermal bridge effect showed that since it is a heat in-heat out on the two flanges and the net heat gain was insignificant compared with the heat received on each side of the web. At this stage of the software development the thermal bridging was omitted from further consideration in the simulation of the stud temperature.

5.2 Temperature effects on loadbearing capacity

Gerlich (1995) investigated the reduction in yield strength and MoE (Young's modulus) of cold-formed steel with increasing temperature (Klippstein, 1978, 1980a, 1980b) and how this would affect the loadbearing capacity of a steel framed wall. The most significant finding was that cold-formed steel, as is used in lightweight steel studs, loses strength and stiffness more rapidly with elevated temperature than does hot-rolled steel. In the temperature range of concern, 400-600^{o}C, the strength and stiffness are 20% lower for the cold-formed steel.

The current design practice is to limit the steel temperature to 400^{o}C. This ensures that the steel yield strength is not reduced to less than about 60% of the ambient values. This is conservative for most applications when comparing the ratio of design load to stud capacity. Limiting steel temperature does not take into account thermal deflections and resulting P-Δ effects. Neither does it consider temperature effects on the modulus of elasticity of steel, which is important to buckling analysis. Limiting temperature is believed to give conservative predictions but the margin of safety is unknown.

The approach adopted, this study, was simply to determine that structural failure, based on a 50% load ratio had occurred when the average stud temperature exceeded 400^{o}C as predicted by the lumped thermal analysis in 5.1.1. Gerlich (1995) was able to show that structural failure was consistently predicted at approximately 70 % of the test value.

A more extensive approach was considered, in this study, using the time-temperature history of the steel framing derived from the model predictions. Structural analysis would then be based on a combination of the axial load and bending, while exposed to elevated temperatures and in accordance with the AISI design manual (AISI, 1991) as modified for temperature effects by Gerlich (1995). Further development of this approach was abandoned, as finite difference analysis would be required and the problems that would be encountered were covered in 5.1.1.

6 Predictive capability of model in fire resistance tests

6.1 Fire resistance tests on light timber frame walls

Three BRANZ loadbearing fire resistance tests on timber stud walls of nominal FRR of 30, 60 and 90 minutes were selected to compare with the models performance. The key parameters are listed in Table 6.1 along with a summary of the results and model comparisons. Individual analyses of each test follow and conclude with an overall summary of the models performance.

Table 6.1: Comparison of selected experimental trials with model predictions for timber framed walls

Trial Number	FR1582B	FR1611	FR1777
Nominal FRR, mins	30	60	90
Wall height, m	3	3	3
Studs, mm x mm	90 x 45	70 x 45	90 x 35
Lining, mm (exp/unexp sides)	9.5 / 9.5	12.7/12.7	16.2/16.2
Lining density, kg/m^3	721	797	862
Lining moisture content %	1	1	1
Insulation	NA	NA	NA
Load, kN per stud	8	2	3
Experimental trial versus model performance			
Fire type/severity, %	ISO/100%	ISO/100%	ISO/100%
Onset of char, mins	15/15	25/23	33/30
Structural failure, mins	42/44	69/61	84/77
Charfactor at structural failure	14/14.1	17.7/18.2	19/19.1
Insulation failure, mins	42/46	69/71	91(NF)/107
Integrity failure, mins	NF/-	69/-	84/-

Note: The model is still in a developmental stage and therefore subject to further refinements. Therefore the results obtained may not be representative of future performance.

The relative performance between the model and the test results is compared in Table 6.2

Table 6.2: Relative performance of the model compared with the test results

Ratio of predicted value to test result.	FR1582B	FR1611	FR1777
Onset of char	100%	92%	91%
Structural failure	104.8%	88%	91.7%
Insulation failure	109.5%	102.9%	117%

6.1.1 Model prediction of fire resistance test of nominal duration 30 minutes

A comparison of the model predictions and the test results are plotted in Figure 6.1.

The temperature of the exposed lining on the cavity side is accurately predicted from the beginning up until the onset of char at 300°C, except that prior to 300°C there is a small divergence followed by a convergence. Beyond 300°C the temperature of the model and test results diverge significantly peaking at about 100°C difference but closing to 50°C at 42 minutes and if the test had continued beyond the insulation failure (42 minutes) then the divergence would be expected to continue.

The temperature of the cavity is similarly predicted with the same pattern, except that at 42 minutes the temperatures closely agree. Prediction of the temperature of cavity side of the un-exposed lining diverges significantly once the temperature rises beyond 100°C; the difference then exceeds 200°C with no apparent convergence until insulation failure occurs.

The temperature of the ambient side of the un-exposed lining, where an insulation failure is deemed to have occurred if the temperature rise exceeds an average of 140°C rise, show a small divergence and then convergence up to 100°C and from there on close agreement till failure (140°C rise) at 42 and 46 minutes respectively for the test and model.

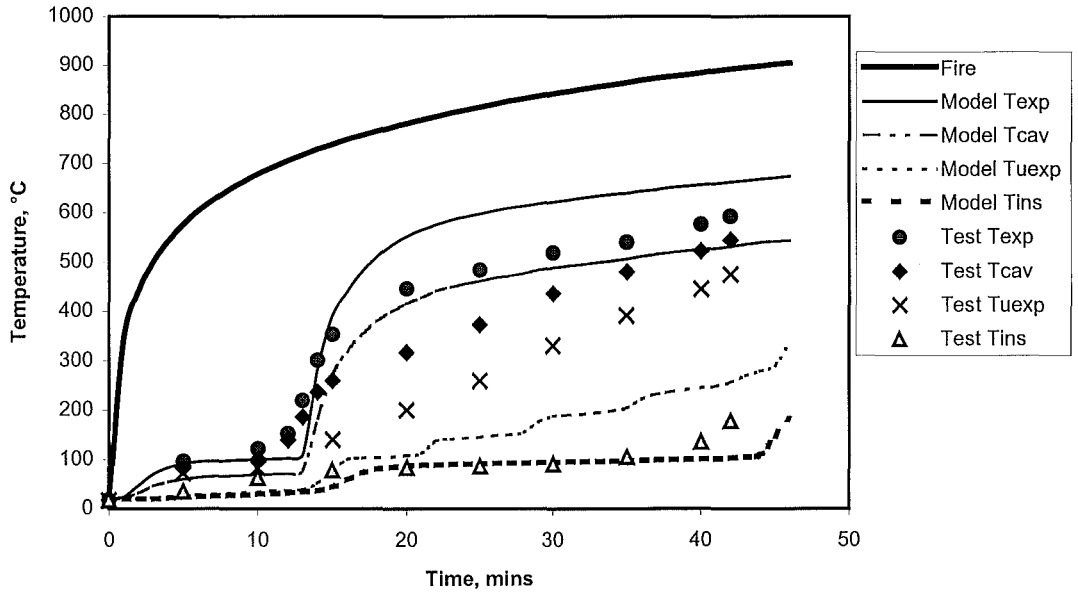

Figure 6.1: Model prediction of temperatures within the wall in FR1582B

The structural failure of the wall is predicted according to Figure 6.2, which shows increase in charfactor from the onset of char at 15 minutes, with increasing charring rate of the studs, and the consequent reduction in the loadbearing capacity of the stud's section is loss due to charring. A failure point is reached when the loadbearing capacity of the studs is reduced below the load that the studs are carrying, signified by the vertical line joining a charfactor of 14 and a load of 8 kN per stud at 44 minutes. This compares well with an actual structural failure at 42 minutes.

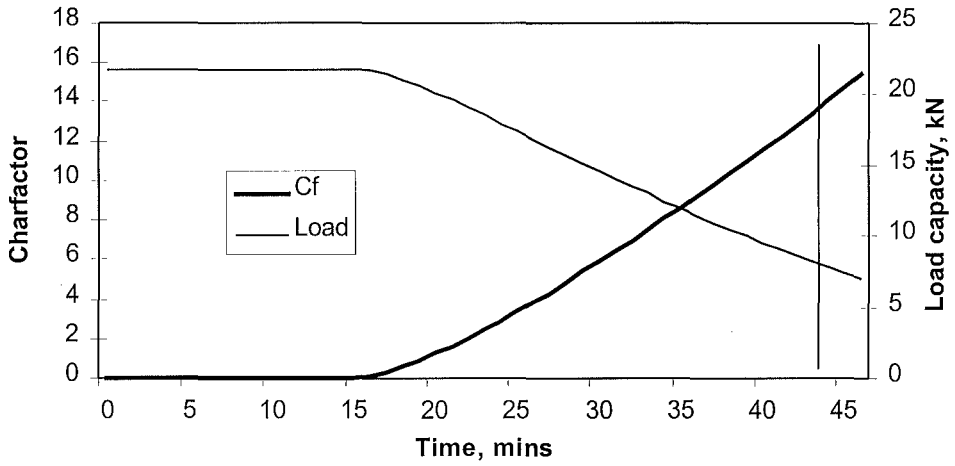

Figure 6.2: Model prediction of charfactor and loadbearing capacity in FR1582B

6.1.2 Model prediction of fire resistance test of nominal duration 60 minutes

A comparison of the model predictions and the test results are plotted in Figure 6.3.

The temperature of the exposed lining on the cavity side is accurately predicted from the beginning up until the onset of char at 300°C, except that prior to 300°C there is a small divergence followed by a convergence. Beyond 300°C the temperature of the model and test results diverge significantly peaking at about 150°C difference but closing to 90°C at 70 minutes and if the test had continued beyond the insulation failure (69 minutes) then the divergence would be expected to continue.

The temperature of the cavity is similarly predicted with the same pattern, except that at 63 minutes the temperatures closely agree. Prediction of the temperature of cavity side of the un-exposed lining diverges significantly once the temperature rises beyond 100°C; the difference then exceeds 200°C with no apparent convergence until insulation failure occurs.

The temperature of the ambient side of the un-exposed lining, where an insulation failure is deemed to have occurred if the temperature rise exceeds an average of 140°C rise,

show a small divergence and then convergence up to 100°C and from there on close agreement till failure (140°C rise) at 69 and 71 minutes respectively for the test and model.

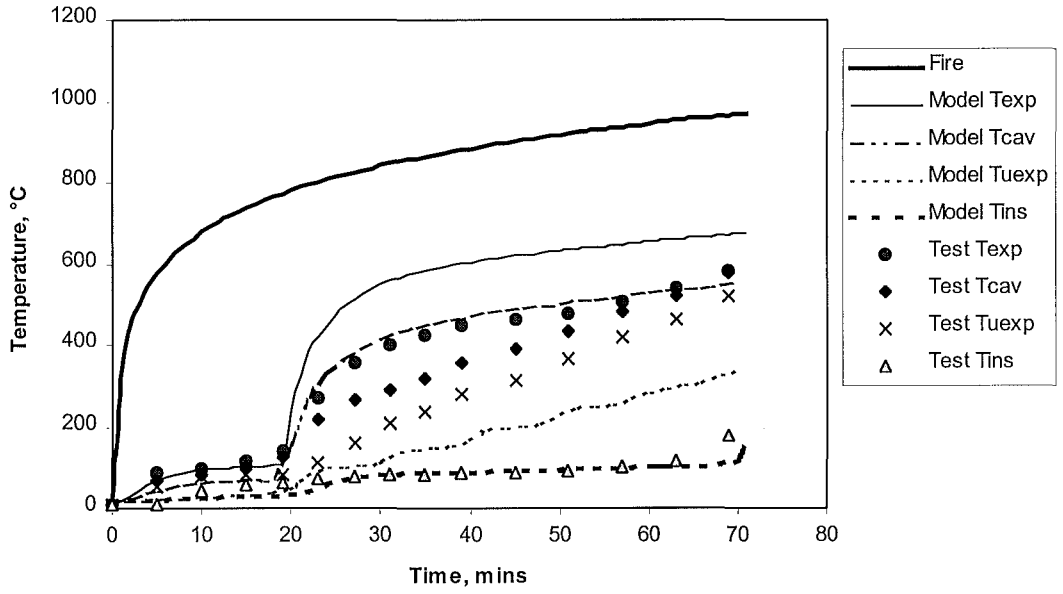

Figure 6.3: Model prediction of temperatures within the wall in FR1611

The structural failure of the wall is predicted according to Figure 6.4, which shows increase in charfactor from the onset of char at 23 minutes, with increasing charring rate of the studs and the consequent reduction in the loadbearing capacity of the stud's section is loss due to charring. A failure point is reached when the loadbearing capacity of the studs is reduced below the load that the studs are carrying, signified by the vertical line joining a charfactor of 18.2 and a load of 2 kN per stud at 61 minutes. Compared with an actual structural failure of 69 minutes this is a conservative prediction.

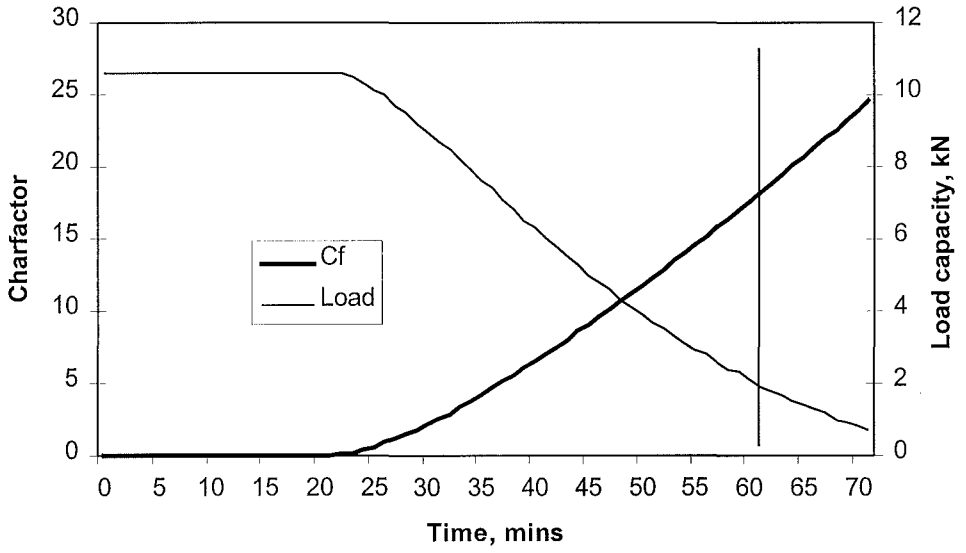

Figure 6.4: Model prediction of charfactor and loadbearing capacity in FR1611

6.1.3 Model prediction of fire resistance test of nominal duration 90 minutes

A comparison of the model predictions and the test results are plotted in Figure 6.5.

The temperature of the exposed lining on the cavity side is accurately predicted from the beginning up until the onset of char at 300°C, except that prior to 300°C there is a small divergence followed by a convergence. Beyond 300°C the temperature of the model and test results diverge significantly peaking at about 175°C difference but closing and crossing over by 85 minutes, at which time the measured test temperature increased to the furnace temperature, an indication that the exposed lining had fallen off.

The temperature of the cavity was not recorded in this test. Prediction of the temperature of the cavity side of the un-exposed lining diverges gradually once the temperature rises beyond 100°C; the difference then increases rapidly coinciding with the falling off (ablation) of the exposed lining.

The temperature of the ambient side of the un-exposed lining, where an insulation failure is deemed to have occurred if the temperature rise exceeds an average of 140°C rise, show a small divergence and then convergence up to 100°C and from there on close agreement up to 85 minutes beyond which the temperature climbed steadily. An insulation failure had not occurred when the test was stopped at 91 minutes for safety reasons due to structural and integrity failures earlier at 84 minutes. The trending upwards temperature of the ambient face indicates that an insulation failure would have occurred in the next 2-3 minutes, long before the 107 minutes predicted by the model, but probably precipitated by the structural and integrity failures.

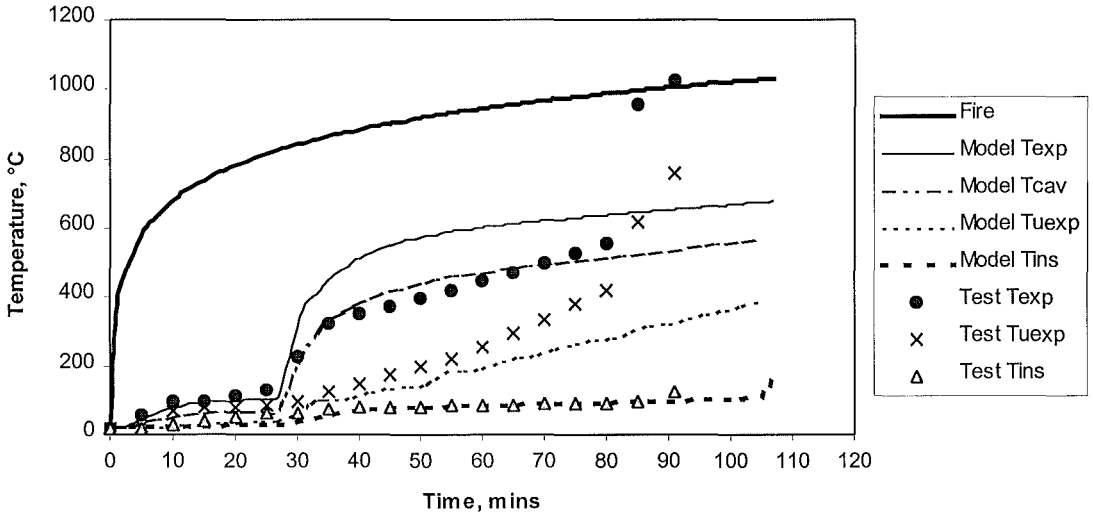

Figure 6.5: Model prediction of temperatures within the wall in FR1777

The structural failure of the wall is predicted according to Figure 6.6, which shows increase in charfactor from the onset of char at 30 minutes, with increasing charring rate of the studs and the consequent reduction in the loadbearing capacity of the stud's section is loss due to charring. A failure point is reached when the loadbearing capacity of the studs is reduced below the load that the studs are carrying, signified by the vertical line joining a charfactor of 19.1 and a load of 3 kN per stud at 77 minutes. Compared with an actual structural failure of 84 minutes this is a conservative prediction.

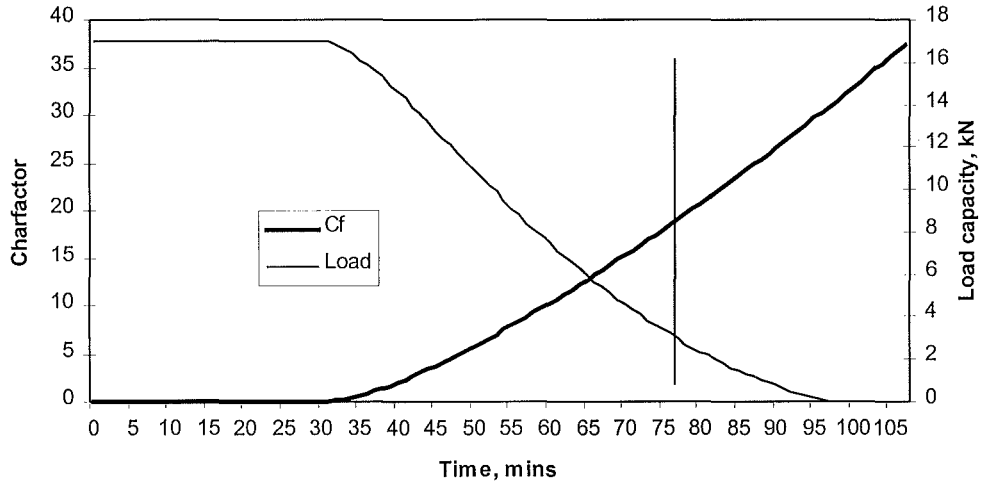

Figure 6.6: Model prediction of charfactor and loadbearing capacity in FR777

6.1.4 Effect of moisture content of gypsum plasterboard on overall performance of system

The moisture content of the plasterboard has a significant influence on the performance of the system as a whole. It is the experience at BRANZ, from years of testing with a large sample of plasterboard types and thicknesses, that moisture content is typically 1%, and this figure is established by drying a sample in an oven at 100°C. Thomas (1997) states that the equilibrium moisture content of gypsum plasterboard is about 4-8%. The differences are no doubt due to different drying regimes, evident by Thomas' drying schedule resulting in the minimum weight being reached at 120°C.

A series of trials using the software model are recorded in Table 6.3, and these show the sensitivity of moisture content to a walls fire resistant performance. Two values are compared, onset of char which is the time required for the cavity side of the exposed lining to exceed 300°C, beyond which the studs are considered to be charring. The other value is the insulation failure time which is the when the ambient side of the wall has exceeded a 140°C temperature rise. Between 0 and 10% the change is quite significant,

especially for insulation failure. In general the results at the lower end of the 1 to 5% range most closely match the test results achieved.

Table 6.3: Variation in performance of specimens with changes in moisture content of lining

	Moisture Content, %	0	1	5	10
FR1582B	Onset of char/Insulation, mins	14/45	15/46	15/47	-
FR1611	Onset of char/Insulation, mins	22/70	23/71	23/78	24/83
FR1777	Onset of char/Insulation, mins	-	30/107	31/111	33/119

6.1.5 Variations between test results and model predictions

Referring back to Table 6.2 the performance of the model can be assessed/summarised on the basis of how closely the performance compares with onset of char, structural failure and insulation failure. These parameters were chosen as they could be considered the most significant in the performance of a fire barrier. Integrity, flaming on the ambient side is another, but the model is not designed to predict this.

In Table 6.2, where the percentage relative to 100% is less than 100% the prediction is considered conservative (under predicted) and greater than 100% the prediction is non-conservative (over predicted). A pattern emerges where the onset of char and structural failure is conservative, if the 30 minute result is ignored. Although it needs to be commented that the closer result with the 30 minute result is because a greater number of model trials have concentrated on 30 minute test results and the model at this stage has a bias for predicting results in a 30 minute time frame. Consequently when the model is then used for the greater time periods differences in the predictive capability are magnified, or the deficiencies are more apparent. The most noticeable of those is the divergence of the structural and insulation predictions.

Improvements in the model aimed at converging the structural and insulation results are planned. The charring model based on the radiation impinging on the stud needs further refinement, as the retardant effects on the charring rate, covered in 4.1.1 have not been fully explored. Reductions in the charring rate can be justified on the basis of density, moisture content, reduced oxygen and perhaps a further reduction due to smoke filling the cavity as the studs char.

Predictions of insulation failure generally tend to be un-conservative and the findings of Thomas (1997) support this. A possible reason may be that models of this type ignore moisture transport within linings and cavities. Moisture transport is a mode of heat transfer by mass transfer; in this case the moisture is evapourated in a hot zone and moves to a cooler zone as steam and condenses giving up heat in the process. This cycle recurs as the temperature front (in the $100^{\circ}C$ range) progresses towards the ambient side. This phenomenon is not so much of a problem in the exposed lining considering that the net result is that the moisture is only evapourated once and the temperature profiles eventually converge. On the un-exposed ambient lining the same cycle occurs but the moisture is lost to the system before an insulation failure, so the modelled heat transfer does not have the benefit of the mass (moisture) transfer to assist in the heat transfer process. For this reason accurately modelling insulation failure is always going to be more difficult. The most practical solution to the problem is probably to tend towards conservative predictions in order to counter this phenomenon, but by how much will be determined by future trials.

Other issues that need to be addressed include the most optimal node spacings, which have previously been shown to influence the results at various milestones in earlier stages of this study. Further elaboration of the influence of node spacings are not reported here as this aspect of the study is still at an early stage and no clear trend has been established.

6.2 Fire resistance test on lightweight steel frame walls

To compare the performance of the model with a steel framed wall, a similar test to FR1611 was selected which used the same 12.5 mm fire rated gypsum plasterboard but with steel studs. This wall was 4 m high and was non-loadbearing with 89 mm x 34 mm x 0.55 mm C-section studs. The data from this test (FR2586) was used to compare with the model predictions of the steel stud temperature at the centre of the web. Figure 6.7shows the modelled temperatures in the wall and superimposed are the predicted steel temperature and the recorded stud web temperature in test FR2586.

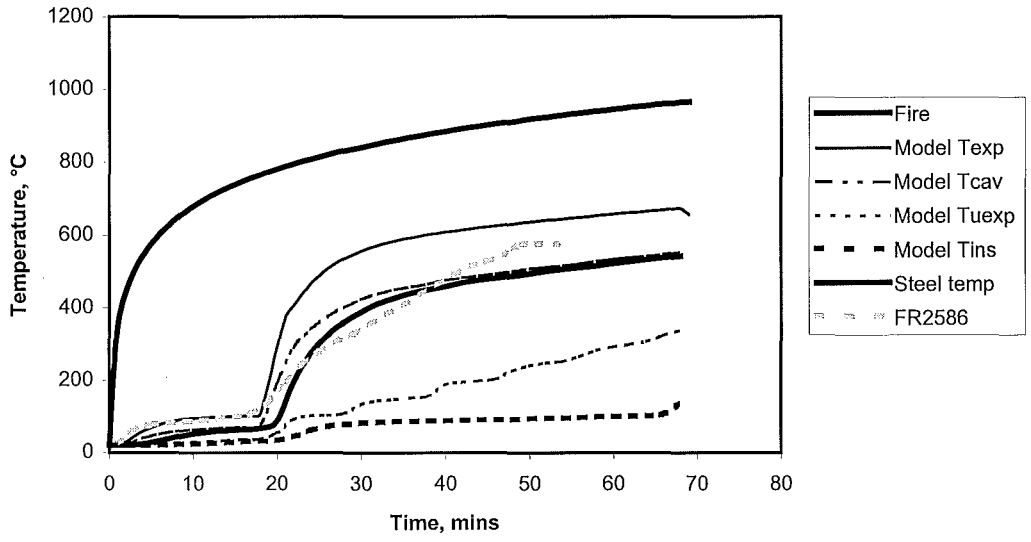

Figure 6.7: Model prediction of temperatures within the wall in FR2586

The modelled steel temperature lags behind the cavity temperature, but the two converge once the rate of temperature rise reduces in the region of 50 to 70 minutes. The measured steel temperature in FR2586 is greater (than the model) up to 22 minutes at which stage the modelled steel temperature is greater up to 40 minutes. Beyond 40 minutes the measured steel temperature is greater and increases at a greater rate than the cavity temperature until the test end. The explanation for this departure lies in the different behaviour, and in particular deflection, of steel walls to timber walls. Timber walls both loadbearing and non-loadbearing generally deflect away from a fire, this is due to the

shrinkage of the hotter exposed side of the stud. If the wall is loadbearing, the load will increase this deflection. Steel framed walls on the other hand deflect towards a fire due to the differential thermal expansion of the studs and a vertical load will increase the deflection. Where it makes a significant difference to the fire performance of wall is in the exposed lining. A timber wall will generally perform better because the exposed lining is compressed and this compression tends to close up the cracks, which develop on heating to fire temperatures. With a steel wall the opposite occurs with the exposed lining in tension and this tends to open up the cracks further. So with a steel wall it is expected that the passage of hot gases from the fire will enter the cavity more easily and earlier increasing the temperatures of the steel studs and cavity. This phenomenon is supported by the observations of the author of a large number of fire tests.

To allow for a steel walls performance disadvantage it is necessary to model the thermally induced deflection and superimpose the applied load using the $P - \Delta$ effect as used by Gerlich (1995) to determine the total deflection expected in a loadbearing wall. Using an estimate of the strain on the exposed lining, caused by the deflection, the increased passage of hot gases into the cavity can be modelled and an adjustment made to the steel stud temperature. Using an approach similar to that described above it is planned implement this effect to differentiate between timber and steel framed walls.

At the models current level of development it can reliably predict the time that an average (middle web) temperature of 400°C is reached. If a stud temperature of 400°C is used as the basis for determining a structural failure as described in 5.2 above, then the model conservatively predicts that failure. Taking Figure 6.7 as an example then a steel temperature of 400°C is exceeded just beyond 30 minutes. Gerlich (1995) tested a similar 1 x12.5 mm lining (on each side) system under loadbearing conditions recording that 400°C for the steel was exceeded at about 30 minutes, structural failure did not occur till 44 minutes by which time the temperature had increased to about 475°C. This indicates the conservatism of using a 400°C limit approach.

6.3 Non standard fires

The majority of comparisons with the model in this project had been with standard fire resistance test fires. For a model to be of use in predicting the performance of fire barriers by fire engineers and designers it has to be proven in a variety of fires of a more realistic nature. Two non-standard fire tests had previously been conducted at BRANZ in an earlier stage of the project and have been compared with the model. A compartment burn with a wooden crib fire load has also been conducted at BRANZ.

6.3.1 Fire tests to non standard fire curves

Collier (1996b) describes two loadbearing fire resistance tests that were conducted to non-standard fire curves. The first one was intended to simulate a ventilation controlled hydrocarbon pool fire with a very rapid growth and rapid decay; the second fire was the opposite with a slow growth and slow decay typical of a surface controlled fire. Each of the fires was intended to be on opposite sides (extremes) of the standard fire curve in terms of time temperature exposure at least up to the point of maximum temperature and the wall exposed to the fire was similar to the nominal 30 minute wall in FR1582B.

It is not intended to report fully the results of the two experiments, except to summarise the modeling comparisons in the growth and decay phases. In the growth phase for both the slow and fast fire exposures the ability of the model to predict the temperatures within the wall was comparable with that of standard fire exposures. Significant differences were encountered in the decay phase the model logically predicted that temperatures within the walls would decrease in phase with the fire temperature. What actually happened was that a secondary fire source developed within the wall cavity as the timber studs continued to burn. Burning of the studs was exacerbated by increased availability of oxygen as air was blown into the furnace to cool the environment in accordance with the predetermined decay curve. While conditions of forced ventilation are somewhat artificial, there is some basis for it by considering a real fire scenario when the fuel source has been consumed down to a level where a ventilation controlled fire reverts back to a fuel controlled fire where there is an excess of oxygen again. To trial this

growth/decay exposure a compartment experiment in conjunction with a floor exposure with fire from above project was designed and is described in section 7.1 onwards.

7 Predictive capability of model in full scale room burn room burn

7.1 Design of compartment

The objective of the experiment with the room burn involved the construction of an ISO standard room with internal dimensions 3600 mm (long) x 2400 mm (wide) x 2400 mm (high) with a door opening at one end of 760 mm (wide) x 2000 mm (high)(Figure 7.1). Construction was of light timber frame, walls and ceiling were lined with a 12.5 mm fire rated plasterboard to give a nominal 60 minutes fire resistance rating. The floor was of 18 mm flooring grade particleboard on nominal 200 mm x 50 mm joists, with 16 mm fire rated plasterboard on the underside, to give a 60 minute FRR system, but when fire attack was from the underside. A check was performed to establish that flashover conditions would be achieved in 6.3.2.1. The fire load in the compartment was required to give the equivalent of a 60 minute (FRR) exposure; the size of the fire load in wood equivalent was determined in 6.3.2.2.

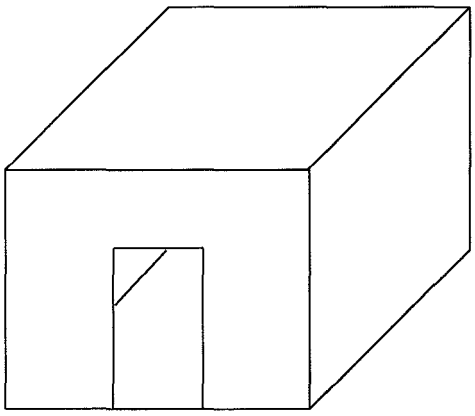

Figure 7.1: General view of compartment

7.1.1 Predicting flashover

Babrauskas' (Walton, 1995) method to determine the heat release required to cause flashover.

$$\dot{Q} = 750 A_o \sqrt{H_o} \qquad \textbf{Equation 7.1}$$

where

A_o =2 x 0.76 = 1.52 m^2, area of opening

H_o = 2 m, height of opening

$$\dot{Q} = (750)(1.52)(2)^{\frac{1}{2}} = 1.61\text{MW}$$

The Method of McCaffrey, Quintiere and Harkleroad for predicting compartment fire temperatures may be extended to predict the energy release rate of the fire required to result in flashover in the compartment, where the flashover temperature is rise is 500°C.

$$\dot{Q} = 610(h_k A_T A_0 \sqrt{H_o})^{\frac{1}{2}} \qquad \textbf{Equation 7.2}$$

where

h_k = effective heat transfer coefficent (kW/m)/K

A_T = total area of the compartment surfaces less openings (m^2)

A_o = area of opening (m^2)

H_o =height of opening (m)

$h_k = 0.03\text{kW/m} \cdot \text{K}$

$A_T = 44.56\ m^2$

$A_o = 1.52\ m^2$

$H_o = 2\,\text{m}$

$$\dot{Q} = 610((0.03)(44.56)(1.52)\sqrt{2})^{\frac{1}{2}}$$

$$\dot{Q} = 1.03\text{MW}$$

Thomas' flashover correlation also calculates the minimum rate of heat release for flashover.

$$\dot{Q} = 0.00852A_T + 0.411A_o\sqrt{H_o}$$ **Equation 7.3**

$$\dot{Q} = 0.00852(44.56) + 0.411(1.52)\sqrt{2}$$

$$\dot{Q} = 1.26\,\text{MW}$$

Using the heat output for flashover as calculated in equations 6.1 to 6.3 it was possible to check that the fire load calculated in 7.1.2 was sufficient to produce the required output for 60 minutes.

7.1.2 Fire load

Law's fire resistance time (Law, 1973) was used to determine the fire load required to burn for 60 minutes (or equivalent) duration.

$$t_{res} = \frac{F_{load}}{\sqrt{A_o A_T}}$$ **Equation 7.4**

where

t_{res} = fire resistance time, mins

F_{load} = fire load in kg wood

or

$$F_{load} = t_{res}\sqrt{A_0 A_T}$$ **Equation 7.5**

$$F_{load} = 60\sqrt{(1.52)(44.56)}$$

$$F_{load} = 494\text{kg}$$

Therefore, 494 kg of wood, rounded up to 500kg was selected as the fire load. This comprised of 9 cribs each weighing between 54 - 56 kg with overall dimensions 550 mm x 550 mm x 1000 mm. The wood selected was untreated pinus radiata rough sawn into 25 mm x 25 mm sections cut to 550 mm lengths and spaced 50mm apart on each layer. Moisture content was approximately 12%. The cribs were stacked two high, and the nine units were evenly distributed around the perimeter of the room, at a distance of 300 mm

from the internal walls. The opening was left clear with a clear view to crib at the back of the compartment, which is where the fire was started.

Taking a heat of combustion for wood of 12 MJ/kg (Babrauskas, 1995)(a conservative figure to allow for incomplete combustion) the total fire load available is:

500kg x 12MJ/kg = 6000 MJ

if this is consumed in 60 minutes the average heat output is

6000MJ/3600secs = 1.67 MW

This compares well with the three figures calculated above indicating that there was sufficient fire load to burn at the rate required for 60 minutes.

The layout of the fire load within the compartment is shown in Figure 7.2 and Figure 7.3.

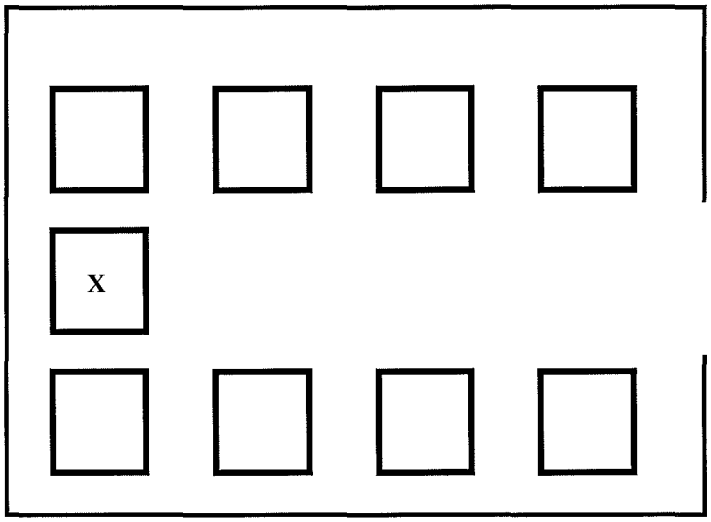

X denotes the location of ignition, crib 1

Figure 7.2: Layout of compartment and fuel load (not to scale)

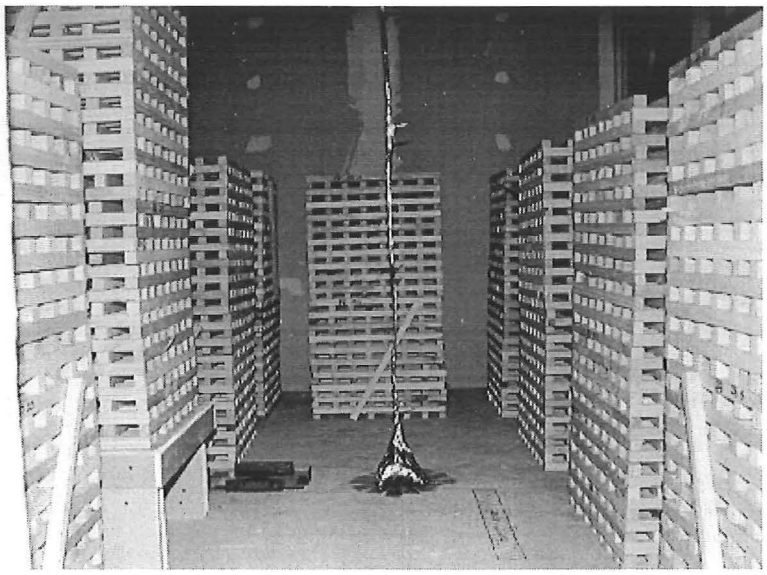

Figure 7.3: Layout of cribs within compartment

7.1.3 Instrumentation

The compartment was extensively instrumented with a total of 103 thermocouples and a heat-flux meter mounted in the floor facing the ceiling. For the walls, floor and ceiling, four thermocouples were mounted i) on the back of the exposed face, ii) in the cavity, iii) cavity side of unexposed face and iv) on the ambient side of the unexposed face. These thermocouples were distributed as follows, three in the floor, five in the ceiling and four on the walls. Three additional thermocouples were mounted on the underside of the flooring only, on one half where the ceiling lining was omitted. The four wall group thermocouples were mounted one on each wall, where one of them was above the door entrance. There were also two thermocouple trees of eight thermocouples each, one at the centre of the compartment and the other in the opening. Finally two furnace grade thermocouples were fixed 100 mm below ceiling height to record the compartment temperatures for the entire burn period, because the thermocouple trees being of lighter construction would not be expected to continue functioning beyond the time that flashover occurred. Thirty sheath thermocouples were included in an instrumented joist for purposes of assessing fire spread down through floors.

For the purposes of this study the data of interest was the temperatures measured in the walls and the fire exposure conditions, which were for a real fire rather than for a standard fire as would be used in a fire resistance test. The data was then compared with the finite difference model prediction of the same fire exposure.

7.1.4 Fire exposure conditions

A commentary of the events that occurred in the room burn experiment is presented in Table 7.1(Whiting, 2000). Figure 7.4 to Figure 7.8 correspond to significant milestones in the development and progress of the fire. The time-temperature for the compartment fire is shown in Figure 7.9, where two recorded thermocouples are compared with the standard (ISO) fire curve. The standard curve is offset 6 minutes and 40 seconds to allow for the delay in the fire developing to more closely match the beginning of significant fire growth. The growth of the fire in this trial was initially slower than the standard fire, but once 500-600^{o}C was exceeded (flashover) the temperature was significantly higher than the standard curve peaking at about 1200^{o}C and some 400^{o}C higher than the standard curve. A stage was reached (800^{o}C) where the rate of temperature rise slowed and continued upwards peaking at 1200^{o}C. This is a region where the fire was ventilation controlled, but even considering that the temperature continued to increase and the reasons for that could include a redistribution of the fire load as each crib was reduced to a heap of glowing embers. The glowing embers, while not necessarily consuming oxygen (in the ventilating air, were contributing to the increasing temperature within the compartment by convection and radiation. Once the available fuel was reduced to a level where the fire became fuel controlled the temperature reduced, settling at a level just above 400^{o}C. At this stage the internal linings had begun falling off, first the ceiling and then the walls exposing the timber frame to the heat and the available oxygen and a small rise in the temperature was recorded.

Table 7.1: Schedule of events, room burn experiment

Time from ignition, minutes	Observations
0	Crib No. 1 ignited.
3	Flaming reaches top of Crib No. 1. (Figure 7.4)
4	First visible smoke emitted from top of doorway.
8	Flaming approximately 0.5m above Crib No. 1.
8.5	Flaming reaches ceiling.
10	Flaming still originating from centre of crib No.1, less than 50% of crib involved. (Figure 7.5)
12	Considerable flaming across ceiling, very clean smoke.
13	Flaming now spread across top timbers of crib No.1.
13.3	Flaming now reaches the sides of crib No.1.
14	Charring visible on top sticks of crib Nos. 2 and 3. (from ceiling jet) Smoke layer through door to 1700mm, white to grey colour. (Figure 7.6)
14.5	Flaming on top of crib No.2, crib No.1 fully involved.
15	Flaming on tops of all cribs, smoke blacker but remains thin.
15.5	Smoke layer through door to 1000, thick black, back wall no longer visible.
16	Entrained air visible drawing light grey smoke back into room at an angle due to wind effects. Flaming spreads across back half of floor enveloping centre thermocouple tree.
16.5	Full Room Involvement. Ventilation controlled, flaming beyond room. Thick black smoke issues from room. Smoke layer within room to 300mm.
17	Flaming across entire floor.
19	Considerable flaming extends beyond room, now pulsing. Smoke layer through door to 900mm.
21	Room lining material falls in small quantities.
23	Flames extend up to 3m beyond room smoke comparatively clear. (Figure 7.7)
25	Whisps of smoke issue from the top of the walls/ceiling assembly junction.
27	Crib No. 9 observed to collapse to floor in door.
30	Failure of the particleboard flooring. Embers fall to ground from under the centre of the room.
30.5	Considerable embers falling, hole in floor approximately 500mm diameter. Ventilation conditions alter significantly.
31	Ventilation condition changes noted in plume, flame extensions less.
33	Large section of floor fails, damaging some instrumentation and taking the heat flux meter with it. Fallen material is extinguished to prevent further instrument damage.
33.5	Flaming externally declines to virtually nil, smoke colour changes to lighter grey/brown.
35	All flaming within room. (Figure 7.8)
36	All cribs reduced to mounds of embers.
38	Half of the floor (unlined side) has collapsed. Flaming breaks out under wall (unlined floor side).
41	Flaming confirmed in all wall cavities.
59	Interior wall linings failing.
65	Back wall linings fall.
67.5	Flaming breaks through to exterior at centre of side wall (lined floor side.)
68	Flaming breaks through to exterior of door wall. Ceiling collapses inwards in centre front (above door).
72	Ceiling assembly collapses in all but one rear corner.
73.5	Ceiling collapses completely.
76	Back wall collapses.
79	Experiment stopped, fire extinguished.

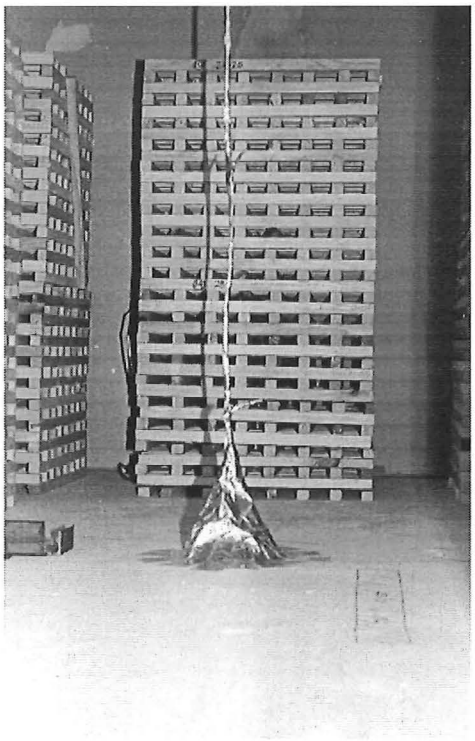

Figure 7.4: Ignition of crib at rear of compartment

Figure 7.5: Initial fire growth in first crib at approximately 10 minutes since ignition

Figure 7.6: Flaming across the top of first crib at approximately 14 minutes

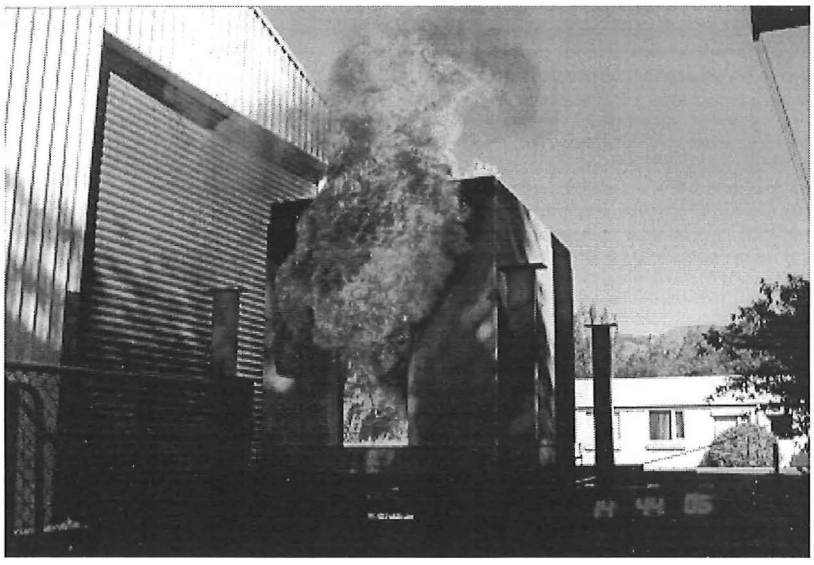

Figure 7.7: Flames extending 3 m beyond room at approximately 23 minutes

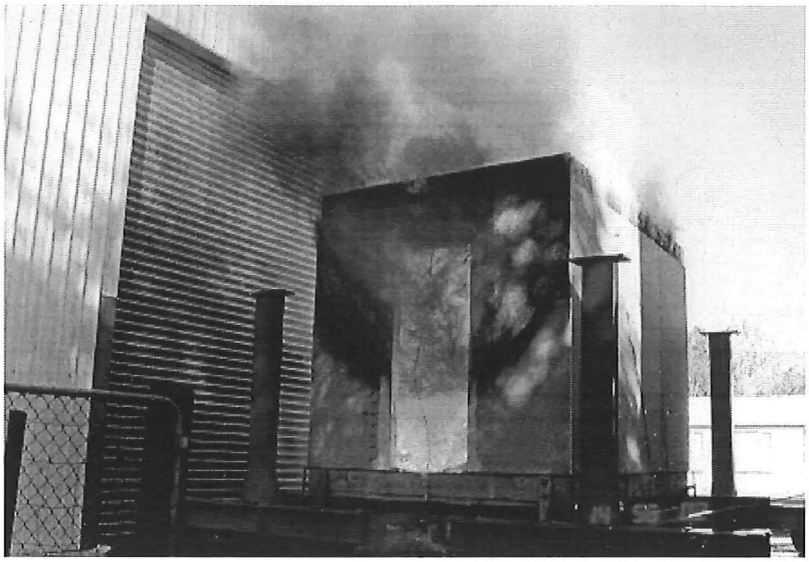

Figure 7.8: Total room involvement, flaming from vent has declined with some smoke now at 35 minutes

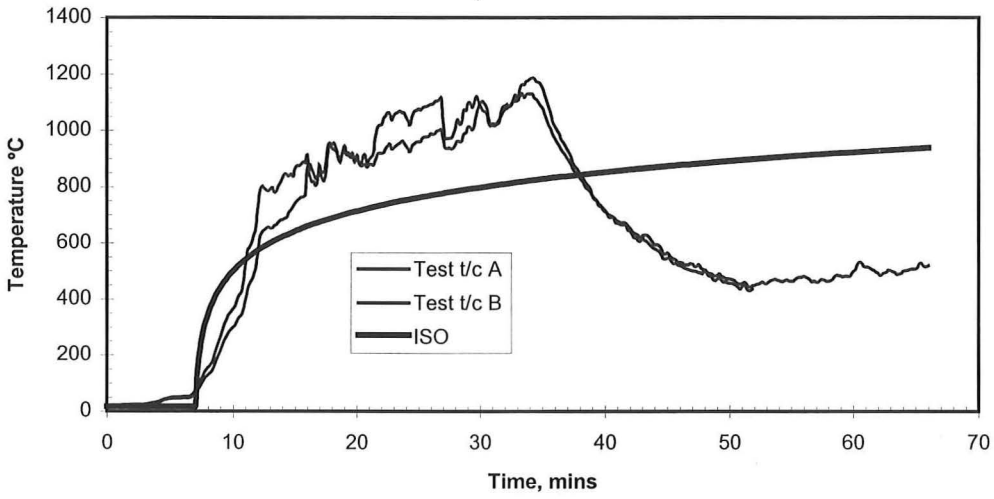

Figure 7.9: Compartment temperatures in room burn

7.1.5 Comparison of the room burn temperatures with the standard fire

Figure 7.9 compares the standard fire the temperatures in the room burn and an explanation is presented in 7.1.4. The time-temperature integrals (area under the respective curves) are compared in Figure 7.10 the graph representing the experiment is an average of test t/c A and B.

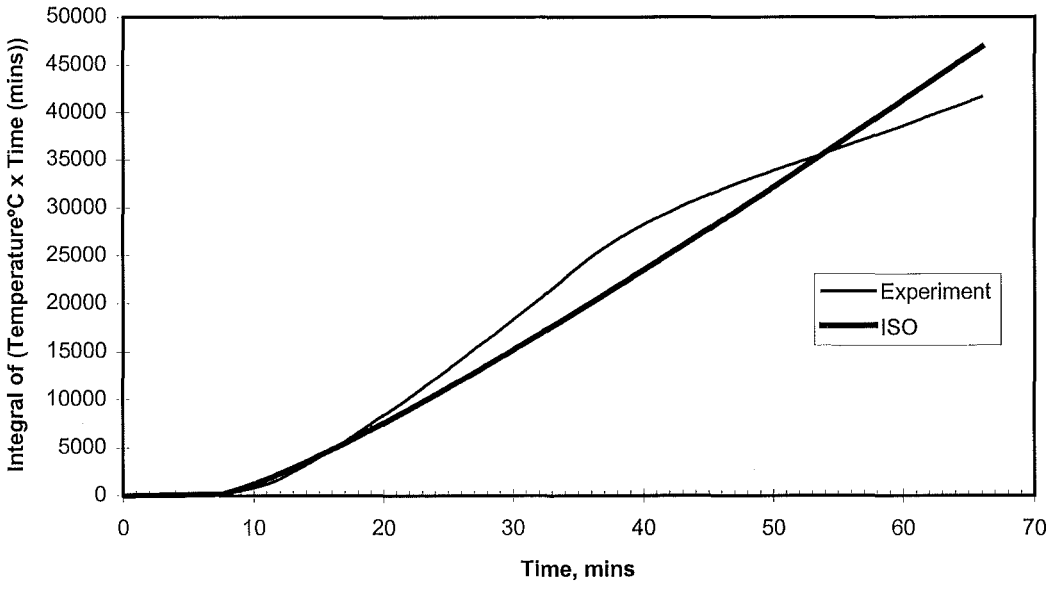

Figure 7.10: Comparison of average room burn temperature with standard (ISO) fire

At 11-12 minutes the compartment temperature exceeded the standard curve and remained above till 38 minutes by which time the fire was well into the decay stage. Integrating temperature rise against time (area under the curves) compares the two fire curves; the graph in Figure 7.10 shows this. From 20 minutes to 54 minutes the severity of the room burn exposure exceeds that of the standard fire curve and it is only well into the decay phase that trend is reversed. It is also evident that the 60 minute fire load, which is only an approximation, produced an equivalent fire exposure approximately

10% less than would have been expected with a standard fire exposure. In light of the assumptions inherent in correlations such as for Law's fire resistance time equations 6.4 and 6.5, where thermal properties of the room boundaries are not considered, 10% variation could be considered an acceptable level of agreement. The size and shape of the vent also plays a significant role, where in the case of the room burn it was observed that a considerable quantity of pyrolysed fuel burnt outside the vent and thus did not contribute to heating within the compartment.

7.1.6 Comparison of the room burn temperatures with a post-flashover design fire

A review of post-flashover fires by Feasey (1999) presented various methods for predicting temperature versus time in post-flashover compartment fires. Based on the COMPF2PC programme a series of graphs such as Figure 7.11 were produced for heavy or lightweight construction and a range of ventilation factors. Within each graph was a family of curves for a range of fire loads.

The fire load and ventilation factor for the compartment used in the room burn are as follows.

$$\text{Fire load} = 500\text{kg x } 18\text{MJ/kg}/(3.6\text{ m x } 2.4\text{ m}) = 1042\text{ MJ/m}^2$$

$$\text{Opening Factor} = A_v\sqrt{H_v}A_T = 0.76\text{m x } 2\text{m x } \sqrt{2\text{m}}/(44.56\text{m}^2) = 0.04824\text{m}^{1/2}$$

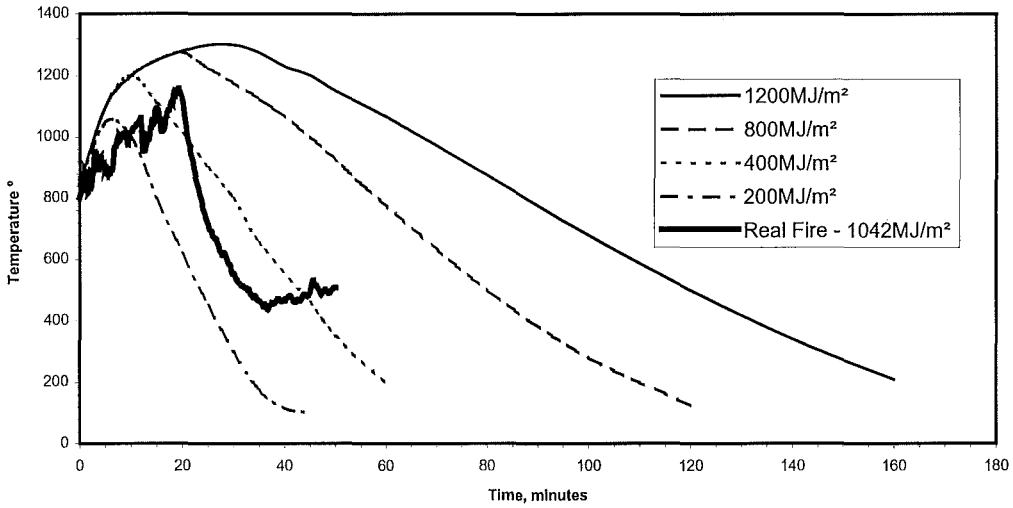

Figure 7.11: Design fires for lightweight compartment construction, ventilation factor 0.04

The graph which best represents the compartment and fire load used is the one reproduced in Figure 7.11, for lightweight construction with an opening factor of $0.04m^{1/2}$ and a family of curves or the fire load ranging from 200 MJ/m^2 to $1200MJ/m^2$. A time-temperature curve representing the compartment fire is superimposed on the graph. It was necessary only to paste in data for the curve once it had exceeded 800°C (at approximately 13 minutes from ignition), for consistency with the other curves. With a fire load for the compartment of $1042MJ/m^2$, it would be expected that the decay period for the room burn would fall between 800 and 1200 MJ/m^2.

Comparing the room burn fire curve with the design fire curves the maximum temperature reached is 1160°C compared with an expected maximum of 1280 to 1300°C, the peak also occurs about 5 minutes earlier. The most significant difference is in the decay phase where the temperature drops rapidly to 450°C and remains at about that temperature until the end of the experiment. The rapid drop in temperature at 20 minutes on Figure 7.11 coincides with the large section of floor falling out at 33 minutes as described in Table 7.1, once the time shift of 13 minutes is factored back in. With a large section of flooring falling out the ventilation factor changes, just how much cannot be

accurately determined. Figure 7.12 (Feasey, 1999) is a redraw of Figure 7.11 with the ventilation factor increased to 0.08 as an estimate of the new ventilation conditions with the hole in the floor. Comparing the decay phase with Figure 7.12 from 20 minutes onwards gives a reasonable comparison, ideally the real fire curve should channel between the 800 and 1200MJ/m^2 curves, instead of starting and finishing in that region but dropping below considerably in between. Of minor significance is the loss of some of the fire load when the floor dropped out, three minutes later (at 36 minutes) it is recorded in Table 7.1 that the wooden cribs have been reduced to mounds of embers, so there was not much fire load left anyway.

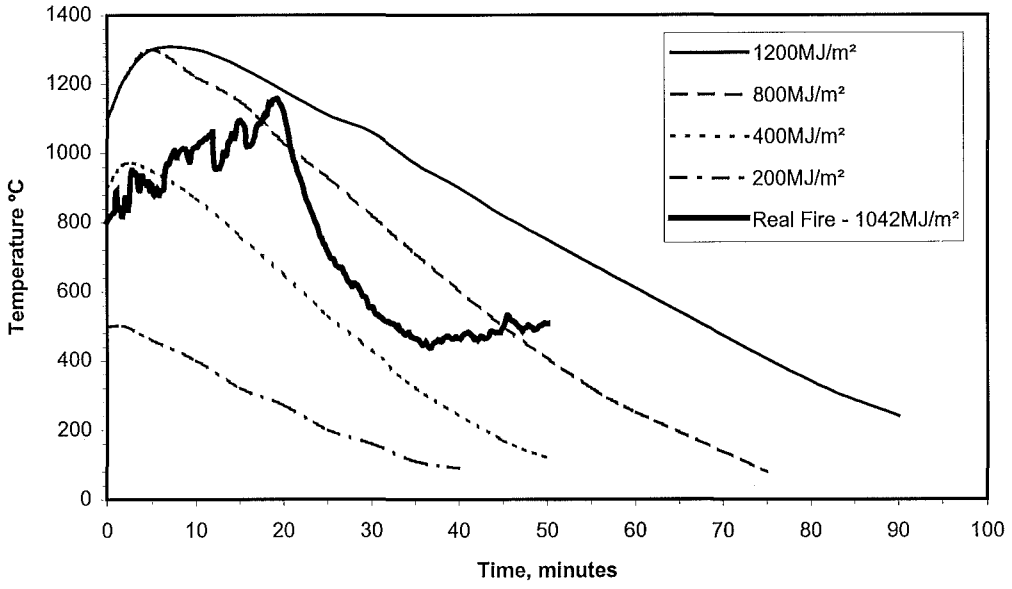

Figure 7.12: Design fires for lightweight compartment construction, ventilation factor 0.08

On the basis of this one result it would appear that the fire curves are conservative, that is the predicted fire exposure is more severe than what occurred in this trial. However, it is worth mentioning that the wood cribs, used as the fire load, showed a tendency to collapse into mounds of embers that continued to smoulder for some considerable time afterwards. It is suspected that a proportion of unburnt wood remained smothered by the ashes and therefore did not contribute any further to the fire. The loss of some of the fire

load when the floor collapsed was not so significant, but the hole in the floor that increased the ventilation is, and would have been more significant if there had been more fire load remaining.

7.1.7 Comparison of measured temperatures with the finite difference model

Comparing the room burn results with model predictions in Figure 7.13, a quite different result is achieved compared with the earlier standard fires. The most significant difference is that the band of temperatures in the cavity, that is the exposed and unexposed lining surfaces and the cavity air temperature, are compressed to a narrow range, compared with the model expectations. This fire scenario is significantly different to a standard furnace test and a possible explanation is as follows. For the temperatures in the cavity to be reduced to a range of 200°C from an expected 500°C indicates that something different is happening in the cavity. Referring the schedule of events on Table 7.1 the entry at 21 minutes indicates that room lining was falling off in small pieces, this is feasible given the more severe thermal shock that the lining was subjected to. It was also noticeable that wind approaching the vent at an angle was entraining smoke back into the compartment, Table 7.1 16 minutes and there was pulsing of the plume from the vent at 19 minutes. A conclusion that the environment inside the room could be described as a well-stirred and turbulent reactor, part of the definition of flashover, and with pulsating pressure was causing the passage of hot gases into the wall cavity through the cracked lining accounts for the narrowing of the temperature band. The entrainment of outside air could also account for the overall lower temperatures in the cavity, which were measured at mid height.

Prediction of the onset of char is conservative at 24 minutes compared with actual time 300°C was exceeded on the cavity side of the exposed lining at 29 minutes. The prediction of the insulation failure is the opposite with no failure being predicted at 66 minutes, but the continued burning of secondary fires within the cavity caused a failure at 65 minutes.

Significant variations also occur when the fire is in a decay phase; the model predicts that temperatures decrease in phase with the fire temperature. What actually happened was that the timber frame within the wall cavity was charring, as the fire decayed as the fuel load had almost been consumed and the fire became fuel controlled again, rather than being ventilation controlled excess oxygen became available, through the cracked lining. This allowed the timber studs to burn providing a new heat source, which increased the temperature within the cavity (afterglow), while the temperature within the compartment, was reducing. In the context of whether the nominal 60 minute firecell survived the 60 minute fire load, it is reasonable to conclude that it did.

Ablation of the exposed lining appears to be more severe in a real fire; this could be due to a greater thermal shock. Future development of the model may require the introduction of a factor for the rate of fire temperature rise as well as just the temperature.

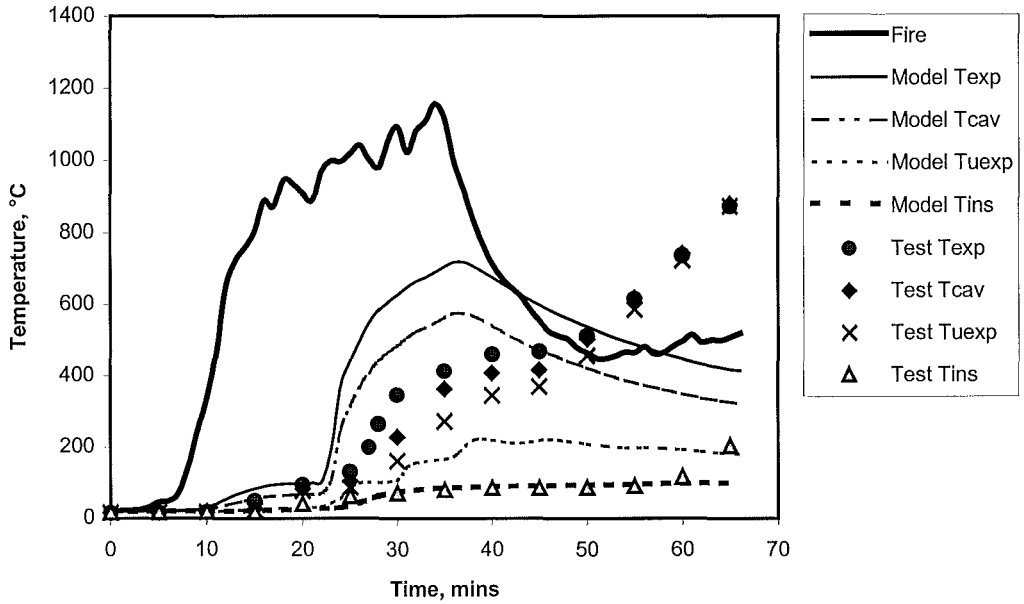

Figure 7.13: Model prediction of temperatures within a wall in roomburn

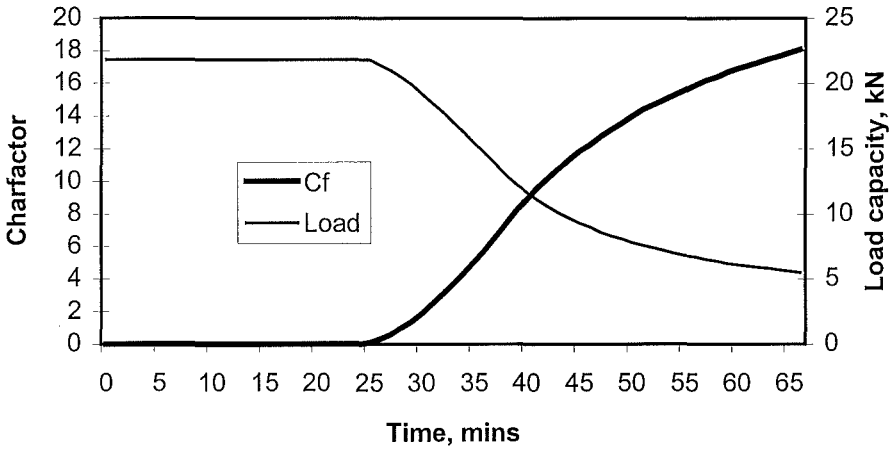

Figure 7.14: Charfactor and load capacity as modelled for roomburn

7.1.8 The effect of fire decay and modelling it

To effectively model the decay stage of a fire several additional considerations are required. The timber studs in the cavity effectively contribute a secondary fire load as may also the paper face on the lining and building paper if present. This would not normally be significant in a fire test where the reduced oxygen content for the duration of the test limits combustion. In a real fire with decay phase the availability of oxygen increases once the fuel load has been largely consumed and ventilation allows an excess of air again. The timber then continues to burn in the cavity as an afterglow, which is easily established due to the timber being dried and pre-heated in the primary fire. An unchecked afterglow will eventually lead to a structural failure because the studs will burn away completely.

To allow for the decay phenomena three options could be considered when modeling a potential fire scenario, which may be a postflashover design fire.

- As a conservative option, continue the fire exposure at the maximum temperature reached until the time period (FRR) has been exceeded without a failure.

- Consider that once the fire load has been consumed and there is no failure, then it has met the required FRR.

- After an equivalent time-temperature integral to the required FRR there is no failure.

If the compartment is constructed of a non-combustible material such as concrete, then a complete burnout of the fire load can be designed for without considering secondary sources of fire.

8 User friendly interface

8.1 Software

The software developed so far performs the calculations described in the preceding text and the future developments and refinements planned are covered in 9.3 under future work.

8.1.1 Inputs

The inputs for the model are illustrated in Figure 8.1. Generally they are self explanatory, but some features warrant some comment as follows:

- The input data is saved to a file for future trials of the same wall system; the output data is also recorded in a file of the same name but with a ".mod" extension. This data is generally used for importing into a spreadsheet for graphics purposes as well as comparing with experimental results if available.

- Parameters of the wall ranging from stud material (timber or steel), dimensions and height to lining parameters and configuration. A drop-down menu and text box for insulation type and density etc are visible if the insulation check-box is checked.

- The fire selection drop down menu includes the ISO standard fire and other real fire time-temperature exposures, which are read from a text file. An input screen for entering additional fire scenarios is planned. This may include a module to enter fire load and ventilation data to determine probable time-temperature curves.

- The command buttons at the bottom of the screen are for file opening and saving, running the model and exiting etc.

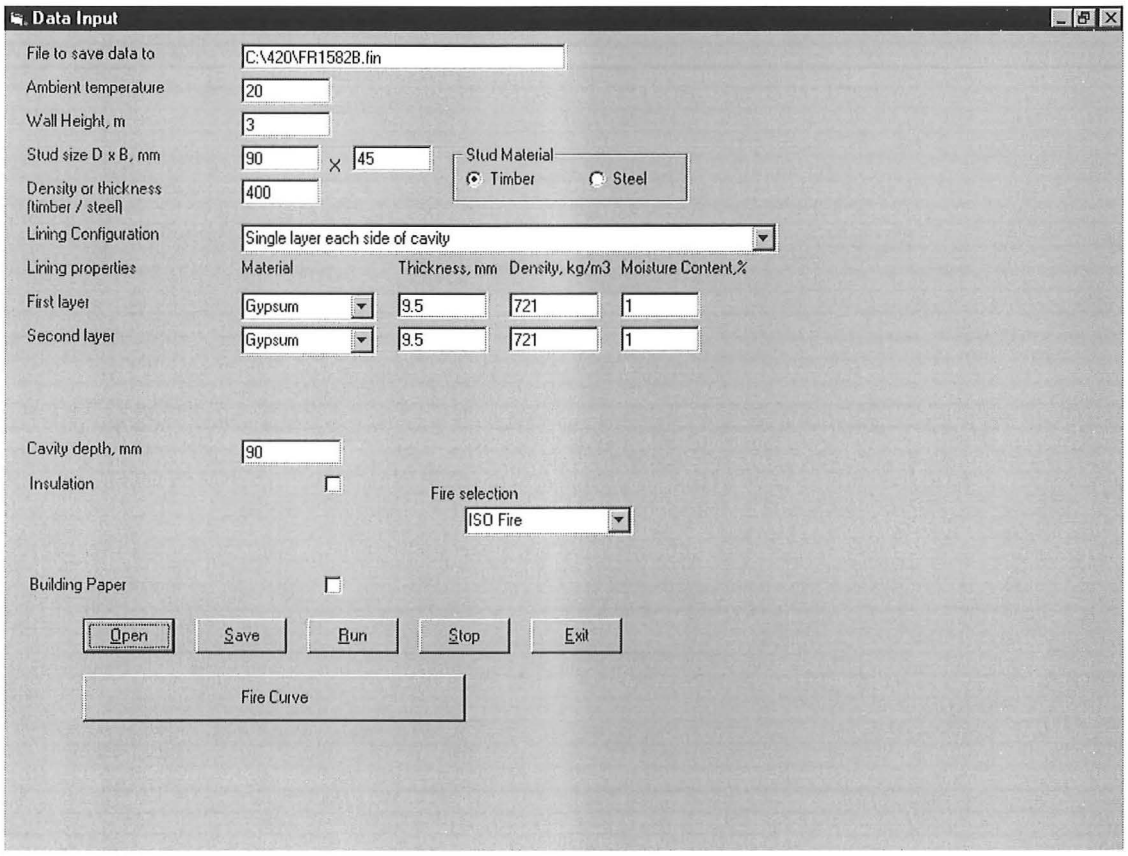

Figure 8.1: User friendly input screen of model for FR1582B

8.1.2 Output data and graphics

Figure 8.2 shows the output screen. In the top left hand corner is a pictorial description of the stud cross section (timber) showing the relative extent of charring with time. The wall performance with time is displayed in the left hand text boxes, onset of char and insulation failure at the time they occurred, the charfactor is updated each minute once the onset of char has been reached. Estimations of the loadbearing capacity and deflection of the wall are also displayed at minute intervals. The temperatures of the fire exposure and within the wall as displayed on the graph and are updated at one minute intervals.

The next stage of development is to include temperatures and load conditions for steel studs.

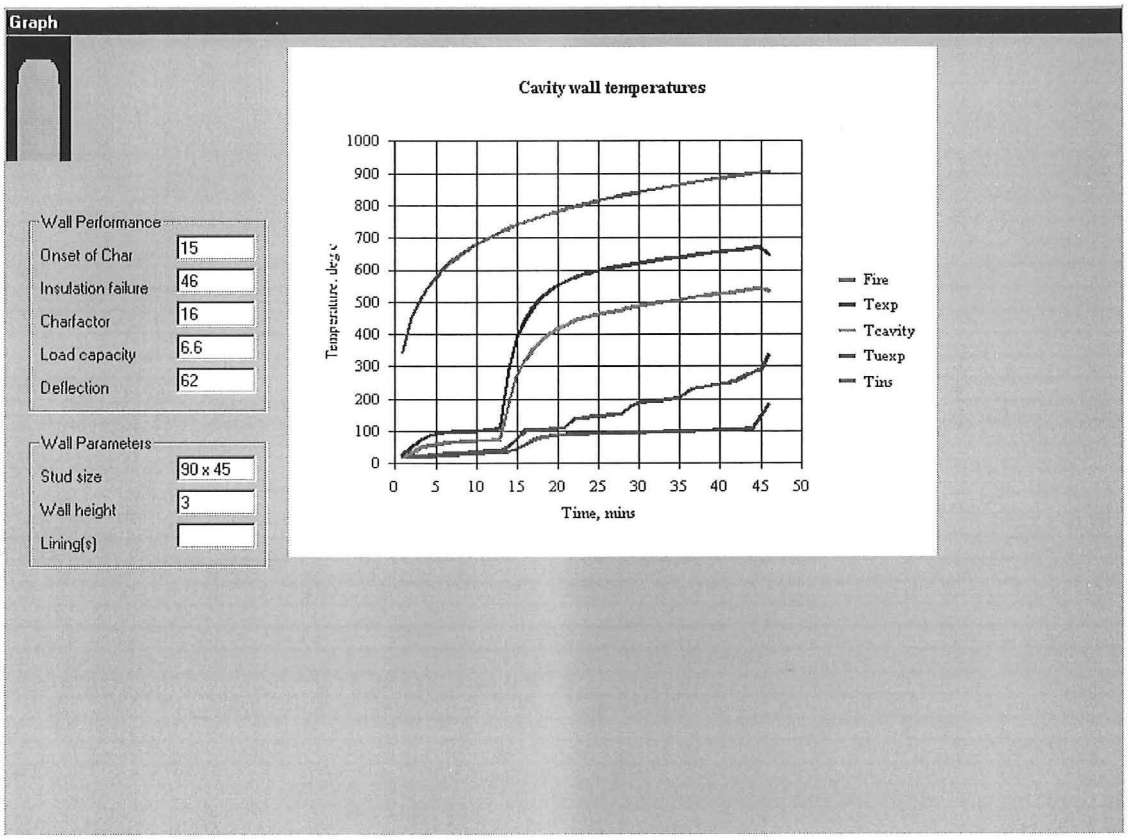

Figure 8.2: Output screen of model

8.2 Applications

Some possible applications for the software, which will be of interest to fire researchers, fire testing engineers and scientists, designers and practicing fire engineers, include:

- Trialling the development of new products before committing to a fire test.

- Simulation of wall behaviour without/before committing to a fire test.

- Allowing designers and fire engineers to investigate the behaviour of established systems when exposed to non-standard fires. Such fire exposure may be based on fire loads and ventilation applicable to specific buildings under consideration.

- As a tool for evaluating opinions on changes to tested systems.

The software will be available for downloading on the BRANZ Internet site and on CD-Rom. The expected availability for a beta version is late 2000 with the finished product in late 2002.

9 Summary and conclusions

9.1 Summary

This report has described the development of a one dimensional finite difference computer model, which, reliably predicts the thermal performance, and insulation failure of cavity walls in both standard and real fires. Building on the thermal response model a charring model for timber reduces the loadbearing capacity of timber studs and a lumped thermal analysis model predicts the temperature of steel studs from which a reduction of the loadbearing capacity and time to structural failure can be assessed.

The moisture content of the gypsum was shown to have a noticeable effect on the enthalpy and therefore makes a small difference to the predictions of structural and insulation failure times.

The charring model for the timber is based on the radiation received by the studs that was emitted mainly from the exposed lining. The rate of charring as well as being proportional to the level of radiation is also dependent on the density and moisture content of the timber and the oxygen content present. Some calibration of the charring parameters is required to match more closely the measured charring and loadbearing capacity determined from a wide range of test results.

The model for predicting the steel temperature, while rather crude, effectively predicts the mid web steel temperature. Improvements can be made by, accounting for the strain on the exposed lining as it deflects towards the fire and opens up passages for hot gases into the cavity. At the moment the test result only exceeds the predicted steel temperature once 400^{o}C is reached and since structural failure is deemed to have occurred at this stage the model can be considered to be satisfactory for this failure criteria. However, if a less conservative solution is required where the steel temperature

is permitted to rise above 400°C then improvements in the prediction of steel temperature and loadbearing capacity will be required.

The experimental trial with the room burn fire established that the model performs similarly given that the actual time-temperature can be used as an input. In a design situation the actual fire exposure would not be known and the input may be based on a post-flashover design curve, which may depend on inputs such as compartment surface area, ventilation and fire load. Indications from the one trial conducted are that the predicted fire exposure might be conservative. The decay phase of a real fire can become significant with secondary fire sources occurring in the wall cavities, but this might not be significant if the fire resistance period required by the barrier has already been exceeded. Another consideration is that by this time the fire service should be in attendance and the fire extinguished.

9.2 Conclusions

The software developed in this project can be used as a design tool that may be used as follows.

- Enable prediction of fire performance of fire resisting systems that are subject to moderate design changes.

- The fire performance of a new system can be checked prior to testing in a fire resistance test, that is a tool for use in product development

- The performance of a system, already established in a fire resistance test, can be predicted in a non-standard fire scenario. This will typically be a slow initial growth followed by a rapid increase to flashover followed by an exponential decay as the fuel is exhausted. Although simulations need not limited to this type of scenario.

9.3 Future work

At this stage of the project there remain several key issues to be resolved in the software. Techniques for addressing some of the following issues are covered in this report and below.

- Ablation: - The layers between the nodes are progressively removed from further consideration, to simulate the wasting away. From fire resistance test results an ablation temperature can be assigned on the basis of the temperature of the cavity side of the exposed face just before a rapid increase in temperature was noted, assumed to be the lining becoming detached from the studs. In a real fire where the temperature rise may be more rapid than a standard fire causing earlier cracking of the lining, some consideration for rate of temperature rise may be required.

- Multiple layers: - Essentially two or more layers with a very narrow air gap between each layer, which causes some, increased resistance to heat flow. Ablation of the lining occurs with the first layer falling off followed by the second and so on.

- Insulation: - A simplified model, ignoring the mass transfer (air flow) within the insulation and thus reducing the problem to one of simple conduction. This assumes the insulation is tight fitting in the cavity without air gaps on any of the edges or faces. A thermal conductivity, density and specific heat for the insulation are required and the heat transfer across the cavity is by conduction instead of convection and radiation. Because the insulation reduces the flow across a wall there will be an increase in the temperature rise in the exposed lining, which may result in earlier ablation of the lining.

- Fire decay: - This can lead to secondary fire sources within the cavity which become significant once the original fire decays as the fuel is consumed. Options

are to attempt to model the secondary fires, or conclude that once a fire is well into the decay phase and if the barriers have not failed, then provided the required fire resistance period has been exceeded the wall has met its FRR requirements.

- Extend the model to cater for floor ceiling systems as well as walls, again making use of and refining previous research as well as information available worldwide.

- Use a neural network technique for optimisation of the software by extensive trialling of various combinations of the leading parameters of heat transfer etc, and comparing the model and test results.

- Distribute model with a user-friendly interface for input of barrier and fire exposure data including runtime graphics and a dump file for output data.

- It is intended to combine this barrier model along with a post-flashover model (yet to be developed) into the BRANZFIRE (Wade, 1998) Zone model. The result will be a zone model capable of developing to post-flashover, which, will then determine whether a fire resistant wall (or barrier) is able to contain a fire for its duration.

10 References

AISI. (1991) 'Load and Resistance Factor Design Specification for Cold-Formed Steel Structural Members'. American Iron and Steel Institute. Washington, USA.

Anderson, L. and Janson, B. (1987) Analytical Fire Design with gypsum – A Theoretical and Experimental Study, Institute of Fire Safety Design, Lund, Sweden.

British Standards Institution (BSI). (1987) Code of Practice for the Structural Use of Timber. Part 4 Fire Resistance of Timber Structures. Section 4.1 Method for Calculating Fire Resistance of Timber Members. BS 5268: Part 4: Section 4.1: 1987. London. United Kingdom.

Buchanan, A. H. (1999) Structural Design for Fire, Department of Civil Engineering, University of Canterbury, New Zealand.

Butler, C.P. (1971) Notes on Charring Rates in Wood. Fire Research Station, Note FR 896. Borehamwood, United Kingdom.

Collier, P.C.R. (1991a) Design of Loadbearing Light Timber Framed Walls for Fire Resistance: Part 1. Building Research Association of New Zealand, Study Report No. 36, Judgeford, Wellington.

Collier, P.C.R. (1991b) Design of Light Timber Framed Walls and Floors for Fire Resistance. Building Research Association of New Zealand Technical Recommendation No.9, Judgeford, Wellington.

Collier, P.C.R. (1992) Design of Loadbearing Light Timber Framed Walls for Fire Resistance: Part 2. Building Research Association of New Zealand, Study Report No. 42, Judgeford, Wellington.

Collier, P.C.R. (1996a) Software for the Design of Light Timber Frame Fonstruction for Fire Resistance - a user's guide version 1.0 Building Research Association of New Zealand, Study Report No. 42, Judgeford, Wellington.

Collier, P. C. R. (1996b) A Model for Predicting the Fire Resisting Performance of Small-Scale Cavity Walls in Realistic Fires. Fire Technology, Vol. 32, No. 2, p. 120-136, 1996.

Collier, P.C.R. (1999) Software for the Design of Light Timber Frame Construction for Fire Resistance - a user's guide, version 2.0. Building Research Association of New Zealand Study Report No. XX. Judgeford, Wellington. (To be published)

Cooke, G. E. M. (1987) Fire Engineering of Tall Fire Separating Walls, FRS4685 D8, Fire Research Station, Borehamwod, United Kingdom.

Cooper, L. Y. (1997) The Thermal Response of Gypum-Panel/Steel-Stud Walls Systems Exposed To Fire Environments - A Simulation for Use in Zone Type Fire Models. National Institute of Standards and Technology, Gaithersburg, MD 20899.

Croft, D. R., and Lilley, D. G. (1977) Heat Transfer Calculations using Finite Difference Equations. Applied Sciences Publishers, Essex, England.

Feasey, R. (1999) Post-Flashover Design Fires. Fire engineering research report 99/6 University of Canterbury, Christchurch, New Zealand.

Fuller, J. J., Leichti, R. J. and White, R. H.(1992) Temperature Distribution in a Nailed Gypsum-stud Joint Exposed to Fire. Fire and Materials, Vol 16, 95.

Gammon, B. W. (1987) Reliability Analysis of Wood Frame Wall Assemblies Exposed to Fire, Berkley, California: University Microfilms Dissertations Information Service, University of California, 1987.

Gerlich, J. T. (1995a) Design of Loadbearing Light Steel Frame Walls for Fire Resistance. Fire engineering research report 95/3. University of Canterbury, Christchurch, New Zealand.

Gerlich, J. T., Collier, P. C. R. and Buchanan, A.H. (1995b) Design of Light Steel Framed Walls for Fire Resistance. Fire and Materials vol 20 No 2 p79-96. 1996.

Harmathy, T. Z. 1995. Properties of Building Materials. The SFPE Handbook of Fire Protection Engineering. Section 1 Chapter 10. Society of Fire Protection Engineers/National Fire Protection Association, Boston, United States.

Klippstein, K. H. (1978). Preliminary Study on the Column-Strength of Cold-Formed Steel Studs Exposed to Elevated Temperatures. American Iron and Steel Institute, Washington, USA.

Klippstein, K. H. (1980a). Behaviour of Cold-Formed Steel Studs in Fire Tests. American Iron and Steel Institute, Washington, USA.

Klippstein, K. H. (1980b). Strength of Cold-Formed Studs Exposed to Fire. American Iron and Steel Institute, Washington, USA.

Law, M. (1973) Prediction of Fire Resistance, Procedings, Symposium No.5, Fire-Resistance Reqirements for Buildings – A New Approach, Joint Fire Research Organisation, H.M Stationery Office, London.

Mehaffey, J. R., Cuerrier, P. and Carisse, G. (1994) A Model for Predicting Heat Transfer through Gypsum-Board/Wood Stud Walls Exposed to Fire. Fire and Materials. Volume 18. pp 297-305.

Mikkola, Esko (1990) Charring of Wood. Espo 1990, Valtion teknillinen tutkimuskeskus, Tutkimuksia-Statens tekniska forskningscentral, Forskningsrapporter- Technical Research Centre of Finland, Research Report 689, 35p.

Perry, R, H., et al. (1997) Perry's Chemical Engineers' Handbook. McGraw-Hill, United Kingdom.

Rogers, G. F . C and Mayhew, Y. R. (1972). 'Engineering Thermodynamics Work and Heat Transfer.' Department of Mechanical Engineering, University of Bristol, Longmans, London

Schneider, U. (1988) Concrete at High Temperatures - A General Review. Fire Safety Journal, Vol . 13, pp 55-68.

Sterner, E and Wickstrom, U. (1990) TASEF – Temperature Analysis of Structures Exposed to Fire. Fire Technology SP Report 1990:05. Swedish National Testing Institute.

Sultan, M, A.(1996). A Model for Predicting Heat Transfer Through Noninsulated Unloaded Steel-Stud Gypsum Board Wall Assemblies Exposed to Fire. Fire Technology, Vol. 32, No. 3, p. 239.

Tien, C, L., Lee, K, Y. and Stretton, A, J (1995) Radiation Heat Transfer. The SFPE Handbook of Fire Protection Engineering. Section 1 Chapter 4. Society of Fire Protection Engineers/National Fire Protection Association, Boston, United States.

Thomas, G. C (1997) Fire Resistance of Light Timber Framed Walls and Floors. Fire Engineering Research report 97/7. University of Canterbury, Christchurch, New Zealand.

Wade, C, A (1998) BRANZFIRE- Technical Reference Guide. Building Research Association of New Zealand, Judgeford, Wellington.

Walton,W. D. and Thomas, P. H. (1995) Radiation Heat Transfer. The SFPE Handbook of Fire Protection Engineering. Section 3 Chapter 6. Society of Fire Protection Engineers/National Fire Protection Association, Boston, United States.

Whiting, P. N. (2000) Behaviour of Light Timber Framed Floors Subjected to Fire Attack from Above. Building Research Association of New Zealand, Study Report (to be published). Judgeford, Wellington.

FIRE ENGINEERING RESEARCH REPORTS

95/1	Full Residential Scale Backdraft	I B Bolliger
95/2	A Study of Full Scale Room Fire Experiments	P A Enright
95/3	Design of Load-bearing Light Steel Frame Walls for Fire Resistance	J T Gerlich
95/4	Full Scale Limited Ventilation Fire Experiments	D J Millar
95/5	An Analysis of Domestic Sprinkler Systems for Use in New Zealand	F Rahmanian
96/1	The Influence of Non-Uniform Electric Fields on Combustion Processes	M A Belsham
96/2	Mixing in Fire Induced Doorway Flows	J M Clements
96/3	Fire Design of Single Storey Industrial Buildings	B W Cosgrove
96/4	Modelling Smoke Flow Using Computational Fluid Dynamics	T N Kardos
96/5	Under-Ventilated Compartment Fires - A Precursor to Smoke Explosions	A R Parkes
96/6	An Investigation of the Effects of Sprinklers on Compartment Fires	M W Radford
97/1	Sprinkler Trade Off Clauses in the Approved Documents	G J Barnes
97/2	Risk Ranking of Buildings for Life Safety	J W Boyes
97/3	Improving the Waking Effectiveness of Fire Alarms in Residential Areas	T Grace
97/4	Study of Evacuation Movement through Different Building Components	P Holmberg
97/5	Domestic Fire Hazard in New Zealand	KDJ Irwin
97/6	An Appraisal of Existing Room-Corner Fire Models	D C Robertson
97/7	Fire Resistance of Light Timber Framed Walls and Floors	G C Thomas
97/8	Uncertainty Analysis of Zone Fire Models	A M Walker
97/9	New Zealand Building Regulations Five Years Later	T M Pastore
98/1	The Impact of Post-Earthquake Fire on the Built Urban Environment	R Botting
98/2	Full Scale Testing of Fire Suppression Agents on Unshielded Fires	M J Dunn
98/3	Full Scale Testing of Fire Suppression Agents on Shielded Fires	N Gravestock
98/4	Predicting Ignition Time Under Transient Heat Flux Using Results from Constant Flux Experiments	A Henderson
98/5	Comparison Studies of Zone and CFD Fire Simulations	A Lovatt
98/6	Bench Scale Testing of Light Timber Frame Walls	P Olsson
98/7	Exploratory Salt Water Experiments of Balcony Spill Plume Using Laser Induced Fluorescence Technique	E Y Yii
99/1	Fire Safety and Security in Schools	R A Carter
99/2	A Review of the Building Separation Requirements of the New Zealand Building Code Acceptable Solutions	J M Clarke
99/3	Effect of Safety Factors in Timed Human Egress Simulations	K M Crawford
99/4	Fire Response of HVAC Systems in Multistorey Buildings: An Examination of the NZBC Acceptable Solutions	M Dixon
99/5	The Effectiveness of the Domestic Smoke Alarm Signal	C Duncan

99/6	Post-flashover Design Fires	R Feasey
99/7	An Analysis of Furniture Heat Release Rates by the Nordtest	J Firestone
99/8	Design for Escape from Fire	I J Garrett
99/9	Class A Foam Water Sprinkler Systems	D B Hipkins
99/10	Review of the New Zealand Standard for Concrete Structures (NZS 3101) for High Strength and Lightweight Concrete Exposed to Fire	M J Inwood
99/12	An Analytical Model for Vertical Flame Spread on Solids: An Initial Investigation	G A North
99/13	Should Bedroom Doors be Open or Closed While People are Sleeping? - A Probabilistic Risk Assessment	D L Palmer
99/14	Peoples Awareness of Fire	S J Rusbridge
99/15	Smoke Explosions	B J Sutherland
99/16	Reliability of Structural Fire Design	JKS Wong
00/1	Fire Spread on Exterior Walls	FNP Bong
00/2	Fire Resistance of Lightweight Framed Construction	PCR Collier
00/3	Fire Fighting Water: A Review of Fire Fighting Water Requirements (A New Zealand Perspective)	S Davis
00/4	The Combustion Behaviour of Upholstered Furniture Materials in New Zealand	H Denize
00/5	Full-Scale Compartment Fire Experiments on Upholstered Furniture	N Girgis
00/6	Fire Rated Seismic Joints	M James
00/7	Fire Design of Steel Members	K R Lewis
00/8	Stability of Precast Concrete Tilt Panels in Fire	L Lim
00/9	Heat Transfer Program for the Design of Structures Exposed to Fire	J Mason
00/10	An Analysis of Pre-Flashover Fire Experiments with Field Modelling Comparisons	C Nielsen
00/11	Fire Engineering Design Problems at Building Consent Stage	P Teo
00/12	A Comparison of Data Reduction Techniques for Zone Model Validation	S Weaver
00/13	Effect of Surface Area and Thickness on Fire Loads	H W Yii

School of Engineering
University of Canterbury
Private Bag 4800, Christchurch, New Zealand

Phone 643 364-2250
Fax 643 364-2758